Survey Paper

A review of train aerodynamics Part 2 – Applications

C. J. Baker
c.j.baker@bham.ac.uk
Birmingham Centre for Railway Research and Education
School of Civil Engineering
University of Birmingham
Birmingham, UK

ABSTRACT

This paper is the second part of a two-part paper that presents a wide-ranging review of train aerodynamics. Part 1 presented a detailed description of the flow field around the train and identified a number of flow regions. The effect of cross winds and flow confinement was also discussed. Based on this basic understanding, this paper then addresses a number of issues that are of concern in the design and operation of modern trains. These include aerodynamic resistance and energy consumption, aerodynamic loads on trackside structures, the safety of passengers and trackside workers in train slipstreams, the flight of ballast beneath trains, the overturning of trains in high winds and the issues associated with trains passing through tunnels. Brief conclusions are drawn regarding the need to establish a consistent risk based framework for aerodynamic effects.

Paper No. 4070. Manuscript received 12 September 2013, accepted 30 January 2014.
Part 1 published in *The Aeronautical Journal*, March 2014, Vol 118 No 1201.
This is the latest in an occasional series of survey articles by leaders in their field focusing on a specific aspect of the aeronautical industry.

NOMENCLATURE

In a publication such as this, with much material taken from published sources, it is difficult to achieve complete consistency of nomenclature. Nonetheless the major notation used is shown below. On many of the figures, information is given in the caption on the parameters shown in the figures.

A	reference area
a,b_1,b_2,c	constants in Davies equation – Equation (1)
a, b	constants in Equations (7) and (15)
a_1,a_2,a_3,a_4	constants in Equation (13)
C_D	drag coefficient
$C_{D,\psi = 0}$	drag coefficient at zero yaw angle
C_{DB}	bogie drag coefficient (Equation (3))
C_{DNT}	nose and tail drag coefficient (Equation (3))
C_F	force coefficient
C_p	pressure coefficient
$C_{RL}(\psi)$	lee rail rolling moment coefficient at yaw angle Ψ
c	characteristic velocity (Equation (14))
$F(t)$	generalised force
f	constant in Equation (14) – overturning fatality rate at reference vehicle speed
h	train height
k	train roughness or Weibull parameter
l	nose length or inter car gap length (Equations (3))
L	train length (Equations (3))
M	vehicle mass
m	exponent in Equations (14)
mp	mean pressure transient
ms	mean slipstream velocity
N	number of services per hour
N_B	number of bogies (Equations (3))
N_p	number of pantographs (Equations (3))
N_p	number of power cars (Equations (3))
N_T	number of trailer cars (Equations (3))
n	lee rail rolling moment exponent
P	train perimeter (Equations (3))
p	pressure transient
R	train resistance (Equations (1)) or comfort condition rank (Equation (16))
Re	Reynolds number
S	length of track section
s	suspension stiffness or slipstream velocity
s_D	standard deviation of delay
s_p	standard deviation of pressure transient
s_s	standard deviation of slipstream velocity
T	length of tunnel
U	total horizontal velocity
u_i	wind velocity at which overturning incident occurs
v	train velocity
v_r	reference train velocity

https://doi.org/10.1017/S0001924000009179 Published online by Cambridge University Press

V	wind velocity relative to the train
x	distance along train from train nose
y	distance perpendicular to track centre line
$y(t)$	lateral displacement
Y	distance of structure from track centre line
α,β	constants in Equations (9) and (19)
γ	constant in Equation (11) that allows for suspension effects etc.
Δ	timetabled difference in tunnel entry time
λ	Weibull parameter
μ_r	human response cumulative probability
Ψ	yaw angle
θ	track semi width in Equation (11)
ρ	air density
Ω	overall risk of an incident

1.0 INTRODUCTION

This paper is the second of a two part review of Train Aerodynamics. Part 1 began by giving a brief historical introduction to the subject and setting the bounds of the review – essentially constraining it to consider only wheel on rail vehicles, and excluding a small number of specialist areas such as train aero-acoustics. It then went on to consider the range of methodologies used in the study of the aerodynamics of trains – specifically full scale and model scale testing and CFD techniques – before considering in detail the flow field around trains. A number of different regions of the flow were identified, and the nature of the flow in each of these regions described. The effects of cross winds and constraints such as embankments and tunnels on these flow fields were also discussed at some length. This paper builds on this consideration of the flow fields around trains to consider a number of current applications of train aerodynamics. In Sections 2 to 8 we consider a range of aerodynamic issues that are of current concern – aerodynamic drag and energy consumption (Section 2); pressure loads on passing trains and trackside structure (Section 3); the effects of slipstreams on waiting passengers and trackside workers (Section 4); the flight of ballast and ice particles beneath trains (Section 5); the effect of cross winds on trains (Section 6); passenger comfort due to pressure transients in tunnels and the effect tunnel micro-pressure waves or sonic booms (Section 7). A brief review is given of other actual and potential issues in Section 8 and some concluding comments made in Section 9. As in Part 1 of this paper what follows draws on the work of previous reviews[1-3], the CEN codes of practice[4-8] and the Infrastructure and Rolling Stock TSIs[9,10].

2.0 AERODYNAMIC DRAG AND ENERGY CONSUMPTION

Traditionally the overall resistance of a train to motion has been required by train designers in order to be able to specify the necessary power of the traction system, and, for electric trains, the power that is required from the electricity supply system. While such calculations are still required, in recent years the focus has changed somewhat, and there is an increasing use of train resistance equations in train simulators to attempt to minimise energy consumption through optimising speed profiles and similarly for timetable optimisation. Whatever the requirement, there is a need to be able to specify the overall train resistance. Conventionally this has been given by the Davis equation[11]:

https://doi.org/10.1017/S0001924000009179 Published online by Cambridge University Press

$$R = a + b_1 v + b_2 V + cV^2 \quad \ldots (1)$$

Here v is the train speed relative to the ground and V is the train speed relative to the air, and a, b_1, b_2 and c are train specific constants. The first two terms are taken to be mechanical resistance terms, the third term is the air momentum drag due to the ingestion of air for cooling and air conditioning purposes, and the fourth term is taken to be the aerodynamic component – i.e. the aerodynamic drag increases with the square of wind speed. This implies that aerodynamic effects will become of increasing importance as vehicle speed increases, and indeed the aerodynamic resistance of trains dominates over mechanical resistance for conventional passenger trains at vehicle speeds greater than around 200km/h, and at 250km/h aerodynamic drag is around 75 to 80% of the total resistance (1). The constant c in the Davies equation can be related to the aerodynamic drag coefficient as follows.

$$c = 0{\cdot}5\rho A C_D \quad \ldots (2)$$

where ρ is the density of air, A is a reference area (conventionally taken as $10m^2$, the approximate frontal area of the train) and C_D is the drag coefficient – the non-dimensional drag in the direction opposite to the train direction of travel. We consider first the case of no cross wind i.e. $V = v$. The drag coefficient itself can, in principle, be divided into a number of components. The first is a pressure drag caused by the pressure differences on the nose and tail of the train and which can be expected to be a function of nose and tail shape – the length / height ratio l/h, degree of streamlining etc. The second component is caused by the pressure difference across the bogies and underfloor equipment and is, to a first approximation, a function of train length. The third component is a friction drag caused by the friction on the train side, roof and underbody. One might expect that this later component would be a function of the Reynolds number (Re) based on train length, and the overall 'roughness' of the train – some sort of integral measure of the irregularities along the length of the train – say k/h. One might expect this last component of drag would be a function of Re^{-n}, where n is of the order of 0·1 to 0·2 for a smooth train and close to zero for a rough train, based on conventional boundary-layer theory. Such a formulation reveals one of the major difficulties in carrying out model scale tests to determine the aerodynamic drag coefficient – the effect of Reynolds number on the friction drag term, which for passenger trains can be expected to be the dominant effect[12]. A further issue with conventional wind-tunnel tests, made without a moving ground, is that the scale of the boundary layer along the ground plane becomes of the same order as train height towards the end of the train, resulting in an unrealistic flow field. A better simulation can be obtained using a moving ground plane, although this still suffers from the Reynolds number issue outlined above, and significant practical difficulties in supporting a long thin model at small heights above a moving ground[13]. Recently work has begun on investigating the use of the moving model technique to obtain aerodynamic drag coefficient, by measuring the deceleration of models along the test track[14], and while these are showing some promise, issues remain concerning Reynolds numbers effects on the friction drag. These points being made, however, standard wind-tunnel tests can be useful in determining changes in drag due to variations in nose shape, addition of fairings etc and have been used in this way by a number of authors[15-17]. Similarly there have been recent studies that have investigated the drag of components of trains using RANS CFD methodologies, including studies to opitmise vortex generator behaviour for reducing tail drag, and for opitmising container spacing[18,19,20].

https://doi.org/10.1017/S0001924000009179 Published online by Cambridge University Press

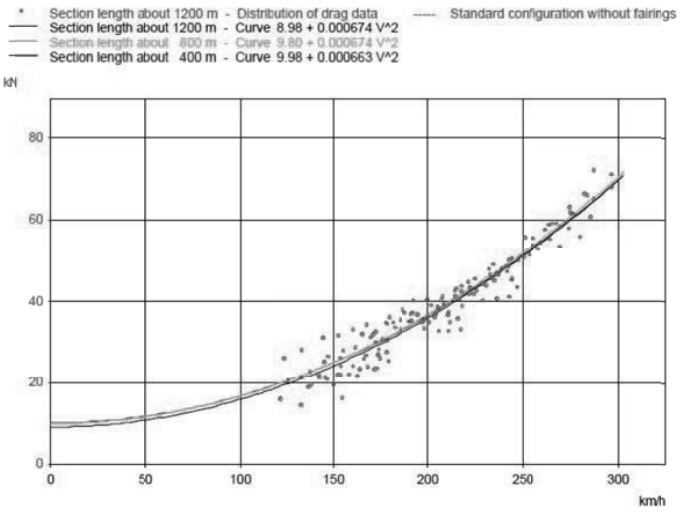

Figure 1. Coasting test to determine train resistance – data and curve fitting[15].

It is because of the difficulties of carrying out physical model tests or CFD trials that the most reliable way of measuring aerodynamic drag remains the full scale coasting test[6], in which trains are allowed to coast to a rest without power from their top speed, and the velocity and distance travelled measured. In an ideal situation, these tests would be carried out on straight, level track, although usually there will be some slope on the track that has to be allowed for. A velocity versus train position function can then be derived, which, through the simple use of Newton's Law, can be converted into a velocity – acceleration/resistance function, which can make allowance for track gradients. A quadratic velocity curve is then fitted to this function and the various components of the resistance thus determined. An example of such a curve fit is shown in Fig. 1[15]. This procedure still depends upon the fundamental assumption that underlies the Davies equation, that the aerodynamic drag is wholly represented in the velocity squared term. The above discussion shows that this cannot be wholly true, as the expected Reynolds number dependence would reduce the exponent of the non-linear velocity term to somewhat below 2·0. Experience with such a methodology also suggests the derivation of the resistance versus velocity equation, which requires a differentiation of the velocity data to obtain the acceleration, is an inherently noisy process which can introduce significant errors, and the fitting of a quadratic velocity curve itself is far from straightforward, with the values of the constants being sensitive to the precise methodology that has been used.

An interesting variant to the above has been developed in Japan using a combination of wind-tunnel tests, measurements of the pressure and velocity variations in running through tunnels and tunnel coasting tests to obtain an alternative estimate of overall resistance (see Fig. 2). This methodology does not however seem to have become widely used[21].

These points having been made, there have been a number of collations of passenger train aerodynamic drag over recent decades, and some of these are tabulated in Table 1 (next page). It can be seen that in general the drag coefficient is most strongly influenced by train length as might be expected, although for a fixed train length, some trains show considerably lower drag coefficients than others. Freight trains, which are not considered in Table 1, inevitably have much higher drag coefficients and are very configuration dependent[22].

https://doi.org/10.1017/S0001924000009179 Published online by Cambridge University Press

Table 1
Compilation of drag coefficient values (* indicates that *b* was assumed to be zero in the curve fit, ** indicates data supplied by Dr S. Hillmansen, Birmingham Centre for Railway Research and Education)

Train	Source	Area (m^2)	Length (m)	C_D – based on an area of $10m^2$
Shinkansen Series 0	11		400	2·65
Shinkansen Series 100	11		400	2·60
Eurostar Class 373	11		400	2·00
Shinkansen Series 200	11		300	1·98
APT-P	1	8·05	294	1·64
ETR 500	15	9·78	250	1·55*
HST	1	9·12	220	1·92
Class 390 Pendolino 9 car	**		218	1·69
AGV 11 car	**		200	1·08
X2-7(Power + 5 coaches + Power)	23		159	1·29
X2000 (Power + 4 coaches + Trailer)	23		139	1·15
ETR 500	15	9·78	119	0·95*
X2-5(Power + 3 coaches + Power)	23		109	1·04
Loco plus 18 coaches	23		356	3·1
Loco plus 9 coaches	23		251	2·45
Loco + Mark II coaches	1	8·80		2·42
Loco plus 5 coaches	23		145	1·80
Loco plus 1 coach	23		40	1·15

In the design of trains it is naturally desirable to be able to predict train drag before the train is built and subjected to coast down testing. A number of nationally based methods exist for doing this, and these are well reviewed by[11] and compared to one another. The UK methodology for Electrical Multiple Units, the Armstrong and Swift method[23], gives the aerodynamic resistance component in the Davis equation as

$$c = 0{\cdot}6125AC_{DNT} + 0{\cdot}00197(PL) + 0{\cdot}0021(pl)(N_T + N_P - 1) + 0{\cdot}2061C_{DB}N_B + 0{\cdot}2566N_p \quad \ldots (3)$$

Here C_{DNT} is the drag coefficient of the nose and tail, C_{DB} is the bogie drag coefficient, P is the train perimeter, L is the train length. l is the inter car gap length, N_T is the number of trailer cars, N_P is the number of power cars, N_B is the number of bogies and N_p is the number of pantographs. The first term represents the nose/tail drag, the second is the skin friction drag and the other terms are the repeating drag terms along the train. A comparison of the results of this method with the results of coast down tests for the Class 373 Eurostar train are shown in Fig. 3 and it can be seen that the use of this methodology results in an over-prediction of the overall resistance[11].

The methods by which train drag can be reduced are in a sense obvious and have been known for many years. These include the following.

- The streamlining of the nose and tail. However, note that for many trains this component of drag is relatively small and the law of diminishing returns applies as the degree of streamlining is increased. Data from Japanese investigators that shows the changes in drag coefficient for nose/tail length/height ratios greater than 2·0 is small[3]. The purpose of the extreme streamlining

https://doi.org/10.1017/S0001924000009179 Published online by Cambridge University Press

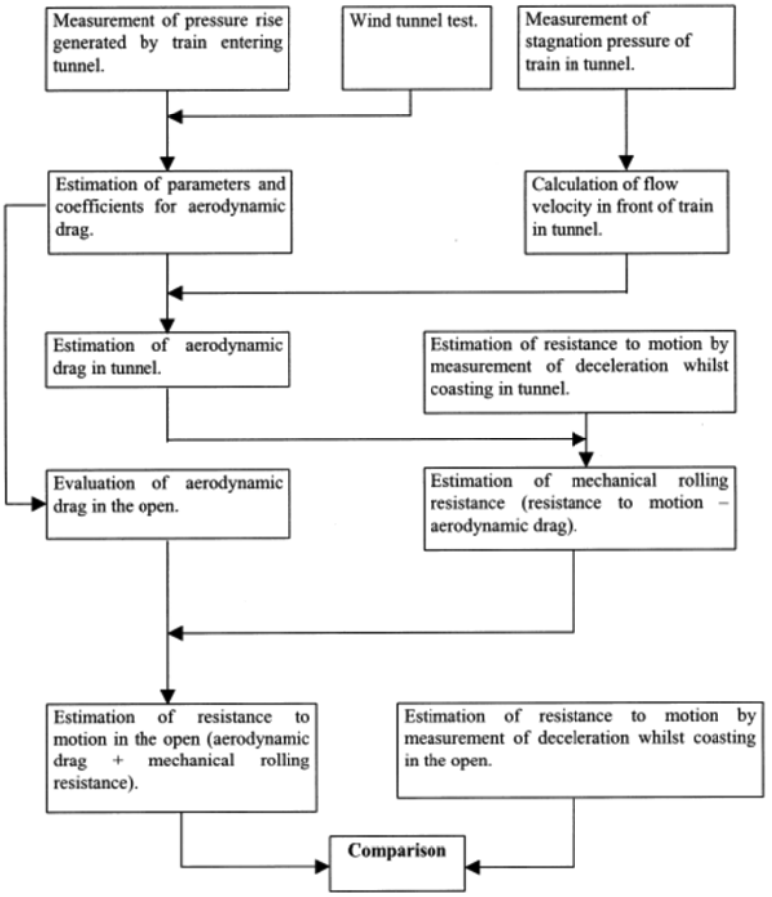

Figure 2. Japanese drag determination methodology[21].

seen on some modern trains is actually to reduce pressure transients in the open air and in tunnels.

- Ensuring the surface of the train is as uniform and free from protuberances as possible. This involves detailed design of door handles, inter car gaps etc. For freight trains, this would involve insuring that, as far as is practically possible, the wagons are as smooth as possible, without discontinuities. This may involve fairings between containers, covers on open wagons etc. It is of interest to note that in the USA, machine vision techniques have been developed to rate the aerodynamic performance of container trains leaving yards, which encourages the yard operator to load trains in the most aerodynamically efficient manner, without gaps between containers etc[24].
- The fairing, as far as practicality allows, of the underbody, so that the roughness is reduced and flow separation around the bogies reduced as far as is possible.

Now the considerations above apply to trains in the open air, in still air conditions, with $V = v$. Now it is clear that in reality trains do not often run in still air conditions, and one might expect the drag coefficient to be affected by crosswinds. A typical variation of drag coefficient with yaw

https://doi.org/10.1017/S0001924000009179 Published online by Cambridge University Press

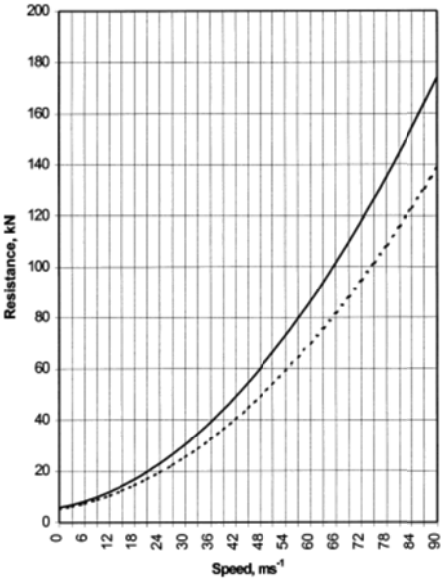

Figure 3. Comparison of experimental resistance results with predictive formula for Class 373 Eurostar (dotted line shows the experimental results, solid line the results of the predictive formula of Equation (11).

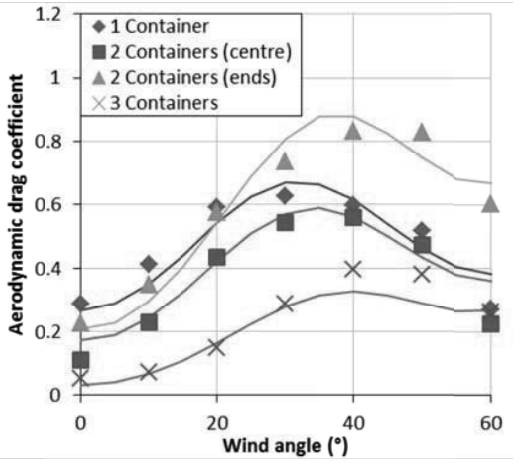

Figure 4. Variation of drag coefficient with yaw angle for container trains[20] (Number of containers refers to position of containers on a wagon that can hold up to three containers. Thus one container is at the centre of the wagon with gaps either side, and three containers fill the wagon completely).

angle is shown in Fig. 4 for a container train[20]. To a first approximation, for small yaw angles, one may write

$$C_D = C_{D,\psi=0}(1 + \alpha\psi) \quad \ldots (4)$$

where ψ is the yaw angle (in radians), and $C_{D,\psi=0}$ is the drag coefficient at zero yaw. Values of α are of the order of 0·5 to 1·0. In Ref. 1 it is estimated that for typical UK weather conditions, the effect of cross winds can add around 10% to the aerodynamic drag term. This effect will be considered further below.

As trains pass through tunnels, it is clear from Part 1 that the flow pattern around the train changes significantly. The energy losses in the flow also change significantly, with the flow between the train and the tunnel wall having to overcome friction on both, and the separation regions around the nose and tail of the train changing significantly. The pressure waves that are created in the tunnel, as they contain energy, also create an effective drag. Very broadly the longer the tunnel, or the greater the blockage ratio, the more the tunnel drag is dominated by friction drag. In two papers in the 1990s[25], Vardy argued that the aerodynamic drag within tunnels has to be considered as the sum of the pressure drag (which includes pressure wave drag) and skin friction drag, and that these two types of drag vary in different ways for different trains and different tunnels. He thus argues that, although an overall drag can be defined, it is not the fundamental parameter. He also makes the point that the area used to define the two components needs to be carefully defined. He defines the term 'aerodynamic area' – the volume of space enclosed by the train divided by its length. In the CEN code[4,5] the approach to allowing for these effects is much simpler and defines a tunnel friction factor, which is used as a multiplier on the open air drag coefficient in the Davies Equation[26].

https://doi.org/10.1017/S0001924000009179 Published online by Cambridge University Press

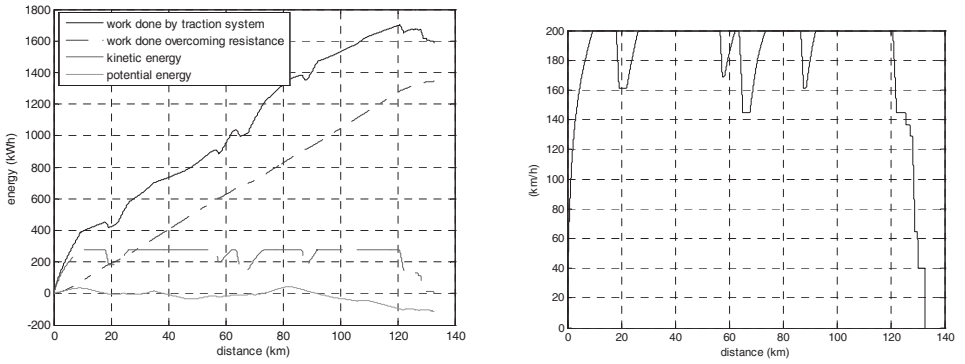

Figure 5. Output from train simulator (The *x* axis shows distance along the route. The *y* axis in the left hand figure shows work done by traction system, work done overcoming train resistance and instantaneous kinetic and potential energy. The y axis in the right hand figure is train speed)).
(Supplied by Dr S. Hillmansen, Birmingham Centre for Railway Research and Education)

Table 2
Train simulator output – energy consumption for standard route plus percentage difference from base case
(Supplied by Dr S. Hillmansen, Birmingham Centre for Railway Research and Education)

	Energy consumption kWh
Base case – Rugby to London non stop	1,588
Base case with C_D + 5%	1,637 (+3·1%)
Base case with C_D + 10%	1,686 (+6·2%)
Base case with C_D – 5%	1,539 (–3·1%)
Base case with C_D – 10%	1,489 (–6·2%)
Base case + 10kph head wind	1,694 (+6·7%)
Base case plus stop at Milton Keynes	1,719 (+8·2%)
Base case plus 50kph running between Milton Keynes and Bletchley	1,655 (+4·2%)

The Davies equation having thus been determined, it can be used in the calculation of train operational performance and energy consumption. Typical output from a train simulator is shown in Fig. 5. This figure shows the performance of a Class 390 Pendolino train running from Rugby to London on the West Coast Main Line in the UK. The speed profile, and the energy consumption is shown. Now Table 2 shows the overall energy consumption for a number of different cases – with the drag coefficient increased and decreased by 5% and 10%, with a 10kph head wind, with one stop at Milton Keynes, and with 50kph slow running between Milton Keynes and Bletchley. From what has been said above, variations in drag coefficient of the order of 5 to 10% represent the uncertainty in its determination, and the variation due to cross winds on a particular journey. It is thus of interest to see that typical operational conditions, with headwinds, unscheduled stops or speed restrictions, cause a variation in the overall energy consumption of the same order of magnitude as would uncertainties in the drag coefficient. Now in train design, there is a desire to obtain the drag coefficient as accurately as possible, in order to be able to specify the required

https://doi.org/10.1017/S0001924000009179 Published online by Cambridge University Press

traction unit capacity, and this can, in the author's view, lead to excessive interest in methods for reducing train drag by a few percent. At a number of points in what follows, the author will argue that, in aerodynamic terms, train design ought not to be separated from considerations of infrastructure and operation. In terms of the specification of train drag the above results suggest something like the following procedure for calculating tractive effort, energy consumption etc.

- Determine the value of the train aerodynamic drag, and other resistances, and assign to each reasonable uncertainties based on the methods that have been used to derive them and thus specify probability distributions for these parameters.
- Specify a typical service pattern for the train, and identify operational uncertainties, such as speed restrictions, and their likely frequency of occurrence.
- Specify a mean wind speed and direction, and the variation of these parameters about the mean i.e. again specify a probability distribution.
- Carry out a large number of train simulator runs, with statistical realisations of the resistance terms, operating conditions and wind conditions, to find a probability distribution of the overall tractive effort and energy consumption.
- Take the design values of these parameters as, say, the mean plus two standard deviations of the probability distribution.
- Such a process would give a context to any changes in drag coefficient that may result from design modifications, and would allow a proper cost-benefit analysis of such modifications to be carried out.

3.0 PRESSURE LOADS DUE TO PASSING TRAINS AND TRACKSIDE STRUCTURE

3.1 Loading requirement

The pressure fields around the trains (and in particular around the front and back of the trains) can result in significant loading on trackside structures (overbridges, walls etc), station platforms and canopies and passing trains. These loads are not usually large enough to lead to instant failure, but repeated loading on structures can cause issues of fatigue, while loading on passing trains can cause significant movement on the suspension system (with resulting passenger discomfort) or can cause ripping of the fabric of soft bodied freight wagons. Clearly some method is required for the specification of such loads. The TSI methodology for measuring train pressure pulses[9] does not fully address this as the measurements are made at specified positions relative to the train in the open air rather than on the surface of a structure, and limit values are set for new trains. These are given by peak to peak pressures of 795Pa for Class 1 trains at 250km/h, and 720Pa for Class 2 trains at their maximum speed. These values are to be measured 2·5m from the track centre line, between 1·5 and 3·3m above the track, during the whole passage of the train (and will thus capture both nose and tail peaks).

In the author's view the setting of the limit values without reference to the effects that pressures cause is a misguided one, but perhaps made understandable by the split between the Rolling Stock and Infrastructure TSIs[9,10], as some methodology is required that can be easily used in train authorisation processes. An earlier methodology in the UK, actually attempted to address this, through requiring measurements of train pressure pulses to be made on stationary trains on

https://doi.org/10.1017/S0001924000009179 Published online by Cambridge University Press

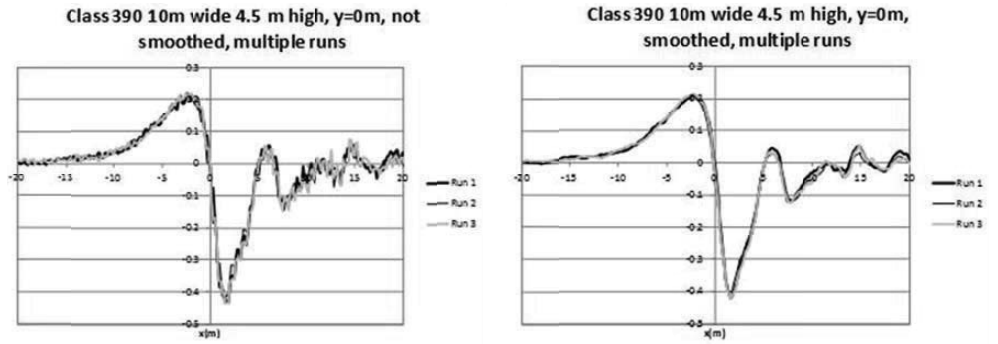

Figure 6. Effect of multiple runs and data smoothing on pressure coefficient distributions for Class 390 train passing an overbridge[27]. (The *x* axis is train position relative to the bridge, whilst the *y* axis is pressure coefficient).

an adjacent track. A limit for the peak to peak pressure transient of 1·44kPa was used, based on tests carried out on the HST in the 1980s. The adoption of the TSI methodology represents, in the author's view, a significant retrograde move.

3.2 Design methodologies

The measurement of loads on structures is an essentially simple process. At full scale, surface pressure taps are installed on the surfaces to be tested, and measurements made with pressure transducers of the required range and frequency response to capture the peak to peak pressure loads. The CEN procedures[6] for this suggest that at least 10 train passes are necessary to enable a suitable ensemble to be achieved. Similar tests can be made at model scale using either static wind-tunnel tests or moving model rigs, with pressure taps on the surface of infrastructure or train models. The CEN methodology for such measurements suggest that, for the moving model tests, at least 10 runs are required in each case with similar speeds and environmental conditions, and the characteristic load then calculated as the mean plus two standard deviations of the peak to peak load ensemble. However, at least for model scale tests, in the author's experience, there is very little difference between the loads from each run of the rig provided that the values are normalised with the square of train speed i.e. put into pressure coefficient form – see Fig. 6 for pressure loads on overbridges[27]. The pressure pulse values can also be accurately obtained from relatively simple CFD methods such as panel methods, or simple RANS based methods.

3.3 Experimental data

Recently the author and his co-workers have carried out a major series of measurements to determine the transient pressure loads on a variety of structures for different trains, using the TRAIN moving model rig[27]. These experiment were made at specifically GB track loading gauges (which are different from those in mainland Europe) with the specific task of obtaining material for a National annex to the CEN code[6]. Some of these results, for trackside hoardings and overbridges, have already been shown in Part 1 Figs 42 and 43, and Fig. 6 in this paper. Part 1 Fig. 42 shows the loading on trackside hoardings at different distance from the track for three types of train – the Class 390, a streamlined 200km/hr train, the Class 158 – a commuter multiple unit and the Class 66 Freight locomotive. It is immediately clear (as would be expected from the results for the pressures and velocities presented above) that the loads due to the Class 66 locomotive are much higher than those of the two other train types. However, the characteristic form of all the load

https://doi.org/10.1017/S0001924000009179 Published online by Cambridge University Press

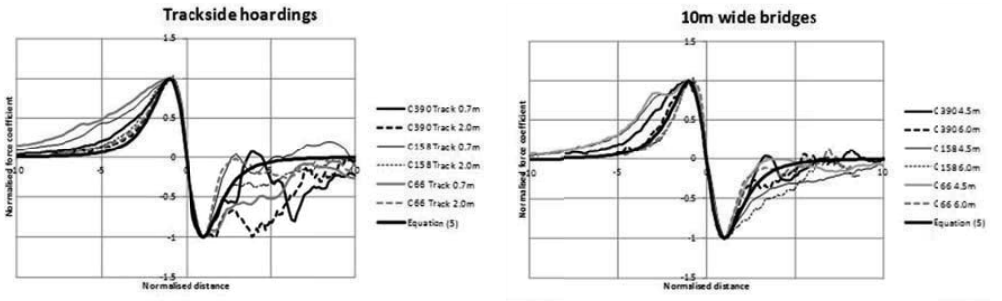

Figure 7. Analytical formulation of loading pressure transients for Class 390, Class 158 and Class 66 vehicles[27]. (The *x* axis is train position relative to the bridge, while the *y* axis is pressure coefficient. The solid line is the analytical curve fit – Equation (5)).

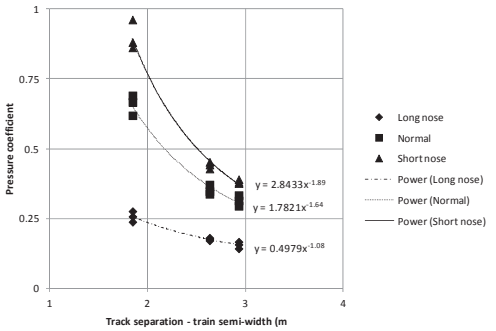

Figure 8. Peak to peak pressure coefficients on an ETR 500 caused by the passing of another ETR 500, with variable nose shape[29] (The *x* axis shows track separation minus train half width. The *y* axis shows peak to peak pressure coefficients).

patterns is similar. An attempt was made to parameterise these using a potential flow analytical formulation[28] as a guide. They found that a useful parameterisation for vertical structures parallel to the track was given by:

$$\frac{C_F}{C_{F\max}} = \frac{x/Y}{(1+(x/y)^2)^{2.5}} \qquad \ldots (5)$$

where x is the distance along the train and Y is the distance of the structure from the track centre line. C_{Fmax} is defined both for the positive and negative peaks i.e. the normalisation is different for positive and negative values of x. Typical results are shown in Fig. 7. While the normalisation is broadly adequate, it can be seen that there are systematic variations for different train types.

With regard to loads on passing trains, moving model experiments that measured the load caused by an ETR500 train with different nose lengths passing a stationary ETR500 for different track spacings have been carried out[29]. Typical results are shown in Fig. 8 for trains with different nose shapes. It can be seen that, as would be expected, the blunter the nose shape the higher the loads, and that the loading falls off as the distance between trains increases.

https://doi.org/10.1017/S0001924000009179 Published online by Cambridge University Press

Note that the fall off has a power law exponent of between 1·0 and 1·6. This is contrary to the exponent of 2·0 that is specified in the description of the work. The difference is probably due to the fact that this exponent was assumed based on earlier work and the data then plotted in a form that fixed it, rather than allowing a free curve fit as above. The use of data such as this is that it can be used to determine acceptable track spacings for new lines, if an allowable peak to peak pressure transient level can be specified. We will turn to this aspect in the next section.

3.4 Loading limits

The loading data discussed in this section is required for two practical reasons. The first is to determine the regular repeated loads on trackside structures to enable ultimate and fatigue loading calculations to be carried out. The second is the loading on passing trains to ensure that the train displacements are acceptable to passengers and do not cause any risk to safety. For the former, the methodology would be to average the loading over a suitable loading length and to transform it into a suitable load effect (eg a bending moment at the base of a barrier). This is broadly the approach taken in CEN[6], where the load is specified as peak maximum and minimum values over a 5m length either side of the zero crossing point for a variety of structures. For vertical structures, it is given in the form of a moment weighted force that can be easily (if confusedly) converted into a base moment. This can be used to either give a maximum design loading for any structure, or through a consideration of train type, frequency and speed, converted into a fatigue load for a specific number of load cycles in a specific time period. It is not really possible to specify limit values in such a case, however, as the design will take account of whatever loading is specified.

The second issue underlies the UK limit mentioned above. Anecdotal evidence suggest that this was adopted in a somewhat roundabout way as being small enough not to cause problems with coffee in cups on the tables in trains. However a rather more rigorous approach could be adopted along the following lines (suggested to the author by Richard Sturt of Arups (private communication).

- For a particular train, being passed by another train, using the experimentally determined pressure transients, calculate the 20m moving average force time history $F(t)$ (assuming that one car of a train is 20m long, this represents the overall force on the car).
- Calculate the displacement of the train on its primary suspension, $y(t)$, from the simple equation.

$$M\frac{\mathrm{d}^2 y(t)}{\mathrm{d}t^2} + sy(t) = F(t) \qquad \ldots (6)$$

  where M is the mass of the vehicle and s is the primary suspension stiffness. For an even greater level of simplicity the stiffness term can be omitted.
- In line with the comments made on other practical applications, such a calculation would best be carried out a large number of times, allowing for uncertainties in pressure time histories, train characteristics and operational characteristics, to calculate a probability distribution of displacement. A limiting value of (say) the mean plus two standard deviations of the displacement could then be compared with realistic values of what might be regarded as acceptable (perhaps one or two centimetres?).

https://doi.org/10.1017/S0001924000009179 Published online by Cambridge University Press

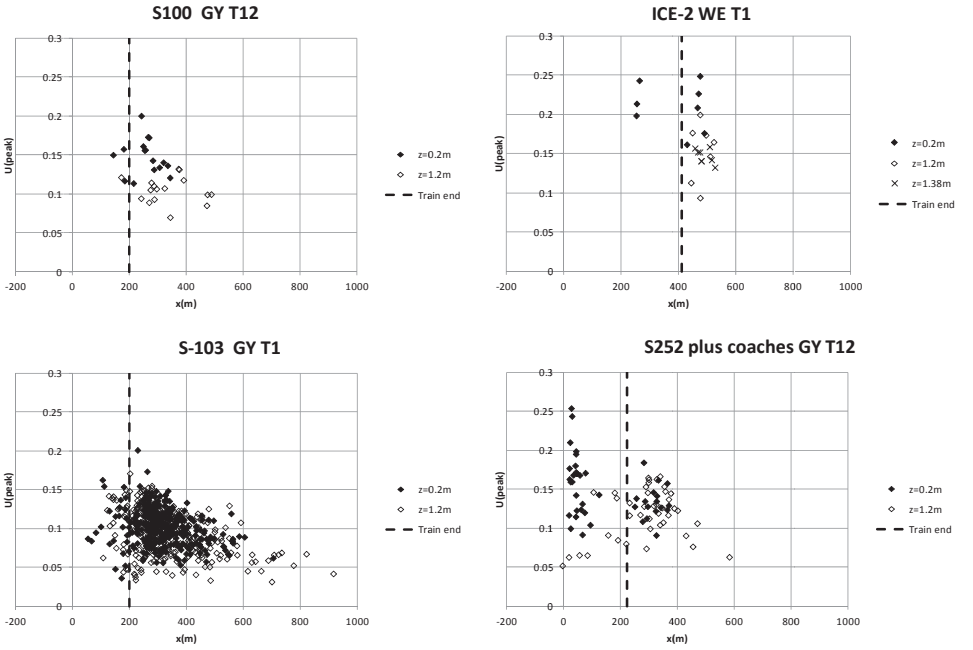

Figure 9. Gust positions and magnitudes for representative train types from AeroTRAIN experiments[31] (The *x* axis of each figure shows the position of the measurement point of the peak velocity relative to the train nose. The y axis shows the normalised TSI velocity).

4.0 EFFECTS OF SLIPSTREAMS ON WAITING PASSENGERS AND TRACKSIDE WORKERS

4.1 The problem

It was shown in Part 1 that the air velocities in the boundary layers and wakes of trains can be significant, and there would seem to be every possibility that these could be dangerous for trackside workers and passengers waiting at platforms. A recent study of such accidents in the UK showed that In the 32 years since 1972, 16 incidents have been reported. Most have involved empty pushchairs although one incident contained a pushchair carrying a child. Minor injuries were sustained by members of the public in two incidents. Three people were almost swept of their feet in other incidents. However, no fatalities have occurred[30]. Thus while the problem does not seem to be a major one, it is a factor that needs to be borne in mind in terms of train and infrastructure design, and will become of increasing concern as train speeds increase.

4.2 Design methodology

In Europe the current methodology for assessing the slipstream risk is outlined in the CEN code[5] and the Rolling Stock TSI[9]. The basis of the method is the determination of a specific characteristic velocity. This has to be obtained from at least 20 full scale train passes with measurements being made at a specific trackside position and at a specified position on a platform. The velocity time histories from these train passes are then averaged with a one second moving average filter, and the maximum value of this averaged velocity obtained for each train pass. The characteristic velocity

https://doi.org/10.1017/S0001924000009179 Published online by Cambridge University Press

is then formed as the mean plus two standard deviations of these gust values. The characteristic velocities are then compared with limit velocities, specified as $22ms^{-1}$ for the trackside position (and thus of relevance to trackside workers) and $15{\cdot}5ms^{-1}$ for the platform position (and thus for waiting passengers). Two points should be noted here however. Firstly within the TSI there are clauses to allow for measurements to be made at those positions historically used in the UK, with somewhat different limit velocities. Secondly a revision to both the CEN code and the TSI, based on the results of the recently completed AeroTRAIN project, is currently in preparation that eliminates the need for platform measurements, and bases both criteria on measurements made at different heights at the trackside position[31].

4.3 Gust measurements

The AeroTRAIN project mentioned above, measured slipstream velocities for a wide range of train types and formations, and was able to specify the characteristic velocity in a much more extensive way than was possible beforehand. These are tabulated in detail in Ref. 31. Typical results for the distribution of gust values for representative trains are shown in Fig. 9. It is notable that the large majority of occurrences of gust maxima are in the near wake of the trains, although for locomotive/carriage combinations, such gusts occur around the locomotive itself. Essentially the characteristic velocity normalised by train speed can be expected to be around 0·15 to 0·20 for streamlined high speed trains, rising to 0·25 to 0·30 for non-streamlined trains. A number of similar measurements have been made using moving model rigs and a comparison between full scale and model scale values for the ICE-2 type train is shown in Table 3[32]. The agreement can be seen to be good, especially when the standard uncertainties of the results are considered, and gives some confidence in the use of moving model experiments to obtain such values.

4.4 The effect of train slipstreams on people

The obvious comment to be made on the above methodology is that it is solely concerned with the slipstream velocities created by trains and does not make any allowance for individual human response. As such it is another example of the design methodology for trains being divorced from considerations of infrastructure and operation. In the RAPIDE project[33], full scale measurements were made of the aerodynamic forces on human dummies and on vertically mounted cylinders with the same frontal area as the dummies, to investigate how the train slipstream velocities were translated into forces (Fig. 10). At the time, the use of a cylinder was a common technique used in assessing the vulnerability of individuals to slipstreams. The analysis was on the basis of a small number of individual time histories of velocity and force rather than on ensemble averages. However the results were somewhat inconclusive, with the cylinders seeming to respond to pressure fluctuations around the nose of the vehicle, and the dummies to velocity fluctuations in the wake, although direct correlation between forces and velocities was not found. On the basis of these results, little confidence could be placed in the use of such techniques, and these methods do not seem to have been pursued further.

Now it is has been shown that the characteristic velocities themselves are subject to significant uncertainties[31], largely due to the underlying physics of the issue, that involves large scale turbulence in train boundary layers and wakes, but nonetheless these values are compared with deterministic limits. The argument can be made that the formulation of the characteristic velocity, as the mean plus two standard deviations of gust values, is a quasi-statistical description, and that the limits themselves are based on the statistical distribution of human reaction, but this is far from explicit and the derivation of these limits is not clear.

https://doi.org/10.1017/S0001924000009179 Published online by Cambridge University Press

Table 3
Comparison of normalised TSI gust measurements between full scale and model scale values for ICE-2[32]

	Height TOR(m)	Distance from track centre(m)	Runs in ensemble	Normalised TSI gust value	Standard un-certainty
RAPIDE full scale	0·5	2·85	7	0·251	±0·024
TRAIN Rig model of RAPIDE experiments	0·5	2·85	7	0·278	±0·026
TRAIN Rig model of RAPIDE experiments	0·5	2·85	14	0·276	±0·018
AeroTRAIN full scale – Track 1	0·2	3·0	11	0·269	±0·020
AeroTRAIN full scale – Track 2	0·2	3·0	32	0·280	±0·012
TRAIN Rig model of AeroTRAIN experiments	0·2	3·0	32	0·276	±0·012

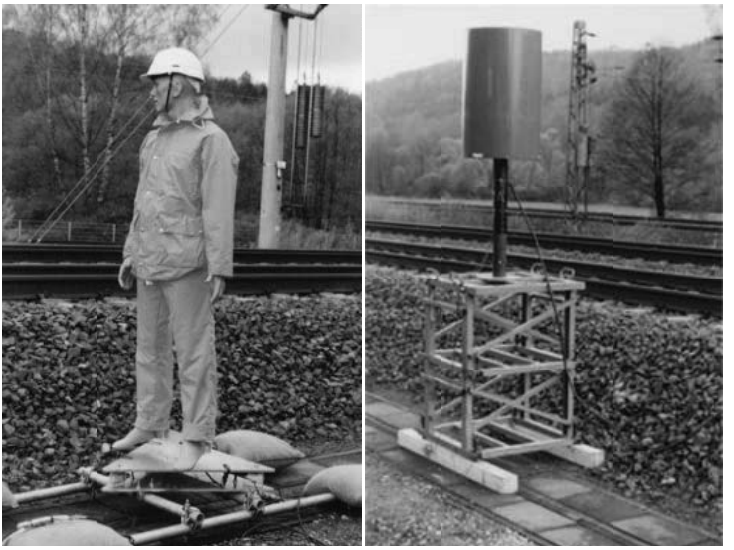

Figure 10. The dummy and cylinder used in the RAPIDE trials[33].

The response of a range of real individuals to different wind gusts has been studied in large scale wind-tunnel tests, through a series of wind-tunnel tests on a range of individuals, and this data used to calibrate models of human behaviour in typical gusts around trains[34]. This experiment and analysis indicates that there is a wide range of human response, with females being more at risk than males to instability in slipstreams, and also suggest that the one second gust value adopted in the TSI is rather longer than it should be. Specifically, however, it allows a cumulative probability distribution of human stability in gusts of different types to be determined – see Fig. 11. In a recent paper[35] the author has proposed the following statistical, risk based methodology for addressing this issue

- Determine from experiments the mean and standard deviations of the one second gust values s, m_s and s_s, and assume a normal probability distribution.
- Determine the cumulative probability distribution for the stability of different categories of people – passengers, trackside workers etc. The data of Fig. 11 suggest this might be of the following form.

https://doi.org/10.1017/S0001924000009179 Published online by Cambridge University Press

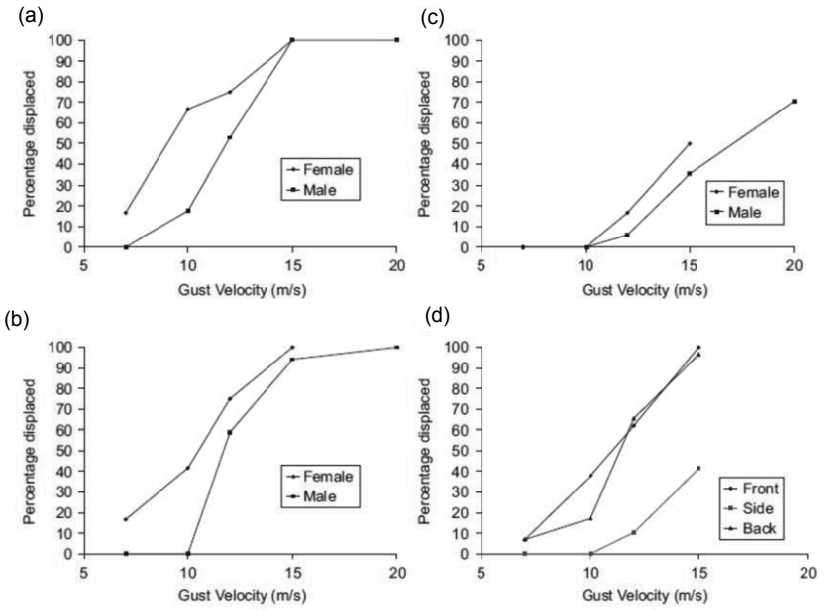

Figure 11. Cumulative distribution of the probability of human instability in sharp edged gusts[34] (The *x* axis shows the velocity of a wind tunnel produced gust, and the *y* axis shows the percentage of displaced subjects, for different gender and displacement categories; (a) facing the oncoming wind, (b) back to the oncoming wind, (c) side on to the oncoming wind, (d) both genders).

$$\mu_r = 0 \text{ for } s < a$$
$$\mu_r = (s\text{-}a)/b \text{ for } a < s < a + b \quad \ldots (7)$$
$$\mu_r = 1 \text{ for } a + b < s$$

a and *b* can be expected to be functions of the assumed gender breakdown of the exposed population.

- Through a convolution of train gust speed probability distributions and the cumulative probability distribution of human stability, calculate the risk of an accident (i.e. a person becoming unstable) for one train passing a particular location. After some manipulation this can be shown to be given by

$$\Omega = \left(0 \cdot 5(1 - erf(^2)) + \frac{1}{^2 \text{-}\pm} \left(\frac{1}{\sqrt{\pi}} \right) (e^{-\pm^2} - e^{-\beta^2}) \frac{\pm}{2} (erf(\pm) - erf(^2)) \right) \quad \ldots (8)$$

where

$$\alpha = \frac{a\text{-}m_s}{\sqrt{2s_s}} \qquad \beta = \frac{a+b-m_s}{\sqrt{2s_s}} \quad \ldots (9)$$

- Through operational considerations, determine the risk of an individual being present on a particular section of track when a train goes by.
- Thus obtain the overall accident risk for an accident to occur on a specific route.

It can be argued that it is more rational to apply limits to the risk levels thus identified, rather than to the slipstream limit velocities themselves – in other words to include a proper consideration of risk within the design process. Clearly, however, further work is required to fully specify the cumulative distributions of human stability in gusts produced by a train, rather than the sharp edged gusts studied in Ref. 34.

https://doi.org/10.1017/S0001924000009179 Published online by Cambridge University Press

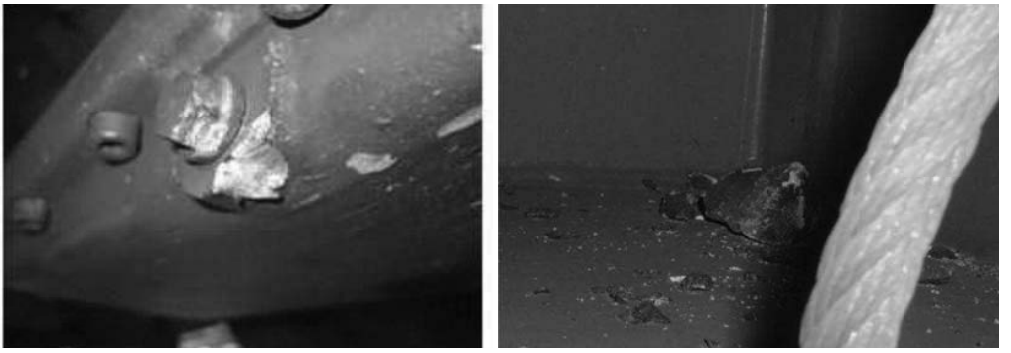

Figure 12. Ballast damage[36].

5.0 THE FLIGHT OF BALLAST AND ICE PARTICLES BENEATH TRAINS

5.1 The issues

The problem of ballast flight beneath trains is one that has made itself felt very forcibly over recent years, with a variety of (usually unpublicised and unpublished) events occurring on high speed lines, where ballast has been lifted from the track, seemingly by aerodynamic effects, and caused considerable damage to train under bodies and tracks. The phenomenon seems to manifest itself in different ways in different countries. In parts of Europe incidents have occurred in normal weather conditions, where large quantities of quite large ballast have become airborne and caused extensive pitting of train under bodies. In particular this occurred during ICE3 tests in French and Belgium lines in 2003 and 2004, where major damage was caused to the trains[36] (Fig. 12), but other incidents have been reported in Italy and Spain. In other parts of France and the Far East, the problem seems to be due to ice particles falling from trains, that then displace ballast that then causes train and track damage[37]. In the UK, the problem appears to be due to smaller ballast particles being lifted onto the track, where they are crushed by either the train that caused the ballast to lift or a following train, leading to pitting of the wheel and rail, and the need for more regular maintenance[38] and shown in Figs 2 in Part 1. Indeed discussion with operators in the UK suggest that the flight of ballast has been a problem for many years, with long term requirements for extra wheel maintenance (through grinding) for the front and rear wheel sets, and regular observations of ballast high up in the under floor equipment during maintenance periods. But without a doubt the most severe issues occur on blasted high speed lines when operating around and above 300km/hr. This phenomenon has initiated a significant amount of research work around the world, particularly within Europe, through the Aerodynamics in the Open Air (AOA) and AeroTRAIN projects. As part of these projects many measurements have been made of the train underbody flow field at full scale and in a variety of facilities at model scale, and equivalent CFD calculations have been made. Some of these have already been reported in Part 1 where the underbody flow field was discussed. In this section we consider the phenomenon of ballast movement itself, and how moving ballast interacts with the induced flow above the track bed.

5.2 Initiation of motion

The first question that needs to be addressed is what are the mechanisms that initiate ballast flight? An obvious way to alleviate the problem would, of course, be to simply ensure that ballast does

https://doi.org/10.1017/S0001924000009179 Published online by Cambridge University Press

Figure 13. Wind tunnel tests on full scale track bed[36].

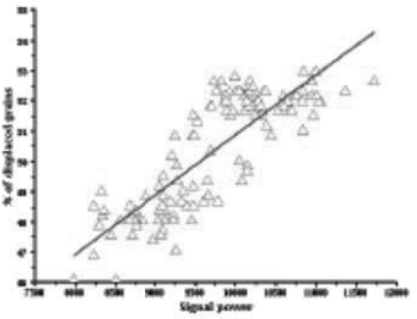

Figure 14. Relation between signal power and percentage of displaced grains[39].

not move at all. Leaving aside for the moment the issue of ice fall from trains, there are a number of possibilities for ballast flight initiation – the vibration caused by the train passing over the track, resulting in a loosening of the ballast; the suction peaks at the front and rear of the train (Part 1, Figs 33)[38], and the shear caused by the velocities under the train. Calculations presented in Ref. 9 suggest that the pressure transients, coupled with the track vibrations may be able to lift small pieces of ballast into the high velocity region above the track, but this should not occur for larger ballast sizes. Extensive work in the recent AOA and AeroTRAIN projects[36] have concentrated on the bed shear stress, or surrogate measurements for this, as the main cause of the initiation of blast movement. The induced velocity increases with height above the bed and one might expect that this effect could become particularly critical where ballast is laid above the height of the sleeper. A series of wind-tunnel tests were carried out to investigate the effects of shear by simulating the underbody of a train within a wind tunnel at a scale of 1:1, subject to a sudden gust, and observing the displacement of ballast – see Fig. 13. From this work the authors were able to conclude that for wind speeds above the bed less than 180km/hr there was no ballast movement, but for wind speeds of 240km/h the majority of the ballast is moving; that lowering the level of the ballast significantly reduces the amount of ballast movement; and that the presence of an intercar gap reduces the ballast movement. Other wind-tunnel tests were carried out at 1/10th scale that allowed the identification of the densimetric Froude number (essentially a non-dimensionalisation of the surface shear stress) as the primary determiner of ballast flight initiation. This parameter has been widely used in other non-rail related studies of aeolian sediment transport. Based on this work a flow parameter was identified that appeared to correlate well with the number of ballast particles moved[39]. This is effectively the square of the instantaneous velocity measured at a suitable point above the ballast bed averaged over the length of the train underbody, and again averaged over an ensemble of train passes. This is effectively a surrogate for a doubly averaged surface shear stress. The correlation of this parameter with the movement of grains is shown in Fig. 14.

In the author's view the multi-variate nature of the problem should not be neglected, and there is a need for further research on the effect on ballast flight initiation of the combined effects of track vibration, pressure transients and shear. It may well be that, for some trains and in some situations, one or other of these effects will dominate, such as in the various experiments described above where surface shear has been identified as being of importance, but a combined consideration is required to enable the phenomenon to be more fully understood, and for all the various effects described above to be put into a common framework. For example, the author and his co-workers recently carried out some exploratory experiments on a short train mounted upside down beneath

https://doi.org/10.1017/S0001924000009179 Published online by Cambridge University Press

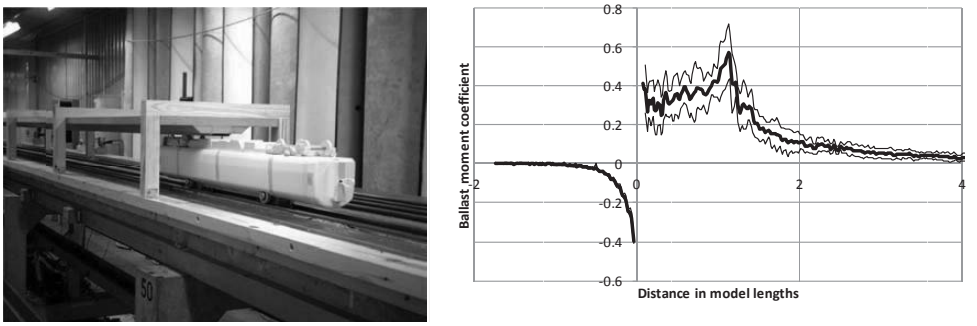

Figure 15. Upside down train on TRAIN Rig (Left hand figure shows a photograph of the experimental set up, and right hand figure shows the overturning moment on hypothetical ballast particles caused by both pressure transients and shear).

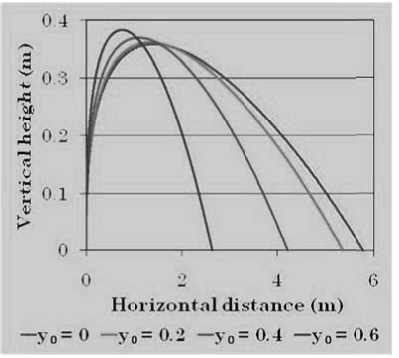

Figure 16. Ballast flight calculations[38] (Curves show ballast trajectory in along track direction for different release points relative to the track centre line).

a representation of the track on the moving model TRAIN Rig, in order to measure in detail the flow field 'beneath' (in this case , above) the train, and in particular the correlations between pressures and velocities – Fig. 15. This enabled the instantaneous overturning moment on ballast particles at the bed to be calculated as the sum of shear (drag) and pressure (lift) forces (although assumptions need to be made concerning the relative contribution of these to the moments). Typical ensemble average results are shown in Fig. 15. The peaks at the front of the vehicle are dominated by pressure forces, while those in the wake of the vehicle by shear / drag forces. While these results must only be regarded as preliminary, and the calculations of moment in some way as quite arbitrary, they do show that it is possible to have ballast moments that are influenced both by pressure and shear forces.

5.3 Flight of ballast

Once the ballast starts to move, it can either continue to 'creep' along the track surface, or, if it has or gains sufficient energy, can 'fly' through the underbody flow region, impacting with either the train or the rail. Quinn *et al*(2010)[38] outlines a method for calculating the flight of ballast in this way, using a formulation that was developed for investigating the flight of wind borne debris during windstorms. Essentially the measured velocity field under the train is used as input to the three dimensional equations of motion for the flight of particles. Examples of flight paths are given in Fig. 16. This work shows that it is quite possible for ballast to either impact on the train

https://doi.org/10.1017/S0001924000009179 Published online by Cambridge University Press

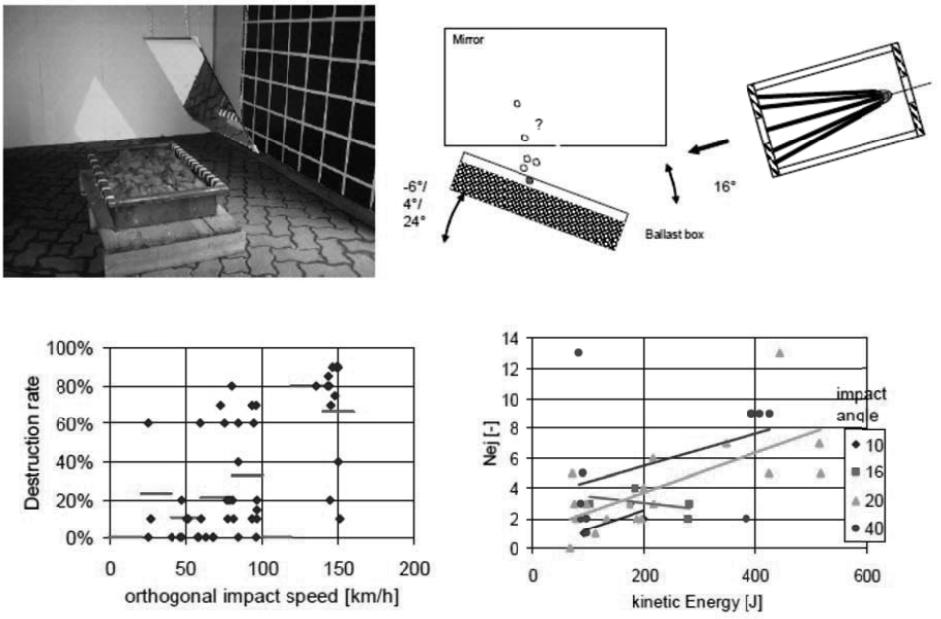

Figure 17. Experiments of ballast projection[40] (Top figures show experimental set up of ballast gun. Bottom left figure shows destruction rate of ballast particles against impact speed. Bottom right figure shows number of particles ejected from bed against impact kinetic energy).

above it or on the rail itself under suitable conditions. More catastrophically, the fall of ice onto the track, or the impact of large pieces of flying ballast onto the ballast bed can initiate a large scale movement of ballast and a chain reaction can take place with significant ballast movement[39,40]. As part of the AOA project measurements were made of ballast projection after impact by high speed ballast particles. Measurements were made of ballast particle destruction, and further ballast ejection. Typical results are shown in Fig. 17. Numerical measurements were also carried out of ballast stone movement, and showed that the initial flight paths of ballast caused primarily by shear were low and flat, but when these impacted on other ballast, there was a certain possibility of much more extensive ballast movement, with much higher and more destructive flight paths.

5.4 Risk and mitigation

Based on the work of the AOA project, SNCF in France developed an outline risk assessment methodology that involves the determination of the 'stress' on the bed caused by the passage of the train given by the mean and standard deviation of the parameter shown in Fig. 14 (essentially a surface shear stress), and the 'strength' of the bed, given by the mean and standard deviation of the number of ballast particles moved at a particular 'stress'[36] The probability of the movement of the ballast can then be calculated from a convolution of the two probability distributions. The former is of course a function of the train type and the latter a function of the track characteristics. This joint consideration of the train and the infrastructure is perfectly consistent with the comments of earlier sections. In more recent work, the authors have taken this further to add into the calculation process the consideration of meteorological conditions and whether or not ice will form, and using this to determine early warning systems to reduce train speeds so that catastrophic ballast flight incidents do not occur[41].

https://doi.org/10.1017/S0001924000009179 Published online by Cambridge University Press

5.5 TSI methodology

The Rolling Stock TSI indicates that in the authorisation of new trains ballast flight should be considered, although it gives (at present) no method for doing so. This issue was addressed within AeroTRAIN and a standard methodology developed by which new trains could be tested. This involves the measurement of the velocities on a standardised section of track (effectively where the ballast is covered by flat sheets) beneath the train being investigated. This effectively enables the shear to be measured, with the ultimate intention that some velocity/shear limits should be specified for new trains. This is a measurement of the 'stress' identified described above. This clearly addresses the issue of large pieces of ballast being moved. Two points arise however. Firstly, where the movement of small pieces of ballast is an issue, as noted above, it would seem to the author that some restriction should be based on the magnitude of the suction peak beneath the front and rear of the train, although no consideration has been given to this at this stage. Secondly this approach is once again moving to a separation of the consideration of train and infrastructure effects. The reader will no longer be surprised to know that the author does not consider this desirable.

6.0 THE EFFECT OF CROSS WINDS ON TRAINS

6.1 The problems

There are a variety of different issues relating to the effect of cross wind on trains. The first, which has received by far the most attention and will be the one discussed at length in this section, is the overturning of trains in cross winds. Such incidents are not as unusual as might first appear and, although the first incident can be traced back to the blowing over of a train on the approach to the Leven Viaduct in Cumbria in the UK in 1903[42]. More recent events have taken place in Japan[43], China[44] and Switzerland[45]. This is an issue that needs to be taken seriously in both train design and route operation because of the major consequences of an accident. A detailed review of the issues involved up to 2009 was presented in Ref. 46. However, there are other related problems – excessive lateral force on tracks due to cross winds[47], gauge infringement (i.e. the vehicle being moved laterally so that it exceeds its maximum allowable displacement)[48] and displacement of the train pantograph with respect to the overhead wire, which can lead to dewirement and possible catenary damage[49]. These issues will be discussed briefly in Section 8.

The first serious study of the stability of trains in high winds seems to have been in connection with the development of the Advanced Passenger Train in the UK in the late 1970s. However, the advent of high speed trains in many parts of the world means that this is an issue that has received attention across Europe and in the Far East. The current situation in Europe is that the Rolling stock TSI requires an assessment to be made of train stability in high winds for all new trains that will travel faster than 160km/h[9]. The methodology for this is given in the CEN code[8], although at the time of writing there is much debate about this methodology and some of the underlying assumptions it contains.

6.2 Outline of methodology

An outline of the methodology used in the train authorisation and route risk assessment processes is given in Fig. 18. It begins with a knowledge of the vehicle design characteristics and the vehicle aerodynamic characteristics. The former usually come from other parts of the design process, while the latter need to be obtained in some way – usually either from wind-tunnel tests of from CFD calculations. This information is then used in some sort of vehicle/wind system model to determine what has come to be known as the Cross Wind Characteristic (or CWC). The vehicle

https://doi.org/10.1017/S0001924000009179 Published online by Cambridge University Press

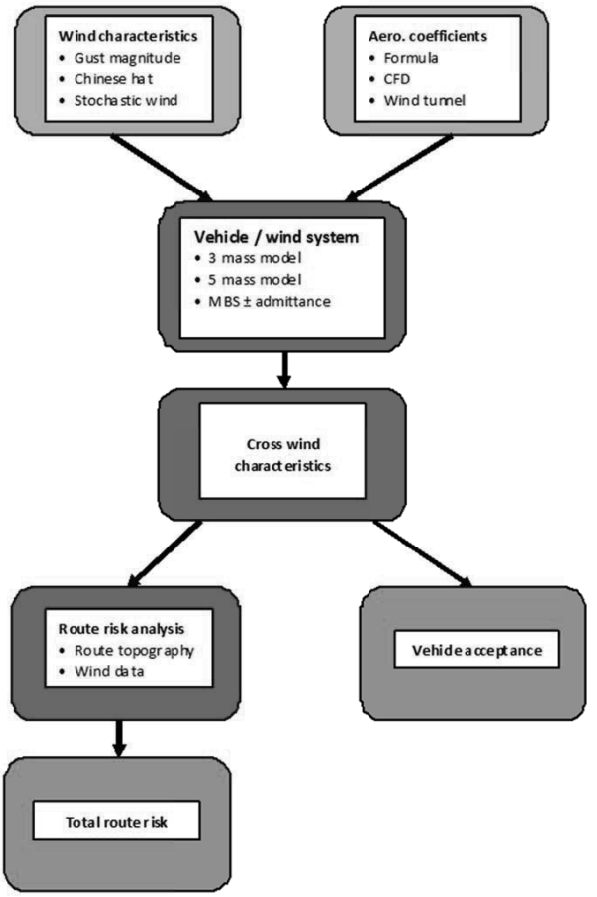

Figure 18. Procedure for determining the risk of trains overturning in high winds.

model can take on varying degrees of complexity, ranging from simple three or five mass models (50) to a full multi-degree of freedom model of the train dynamic system[51]. Similarly the wind can be specified with varying degrees of complexity – through simply the specification of a maximum gust value, through the specification of a standardised gust shape (the so called Chinese Hat gust), to a full simulation of the stochastic wind time history[52], together with some form of admittance function that allows for the lack of correlation of turbulence gusts over the surface area of the vehicle[53]. The CWC derived from these methods is effectively a plot of the wind gust speed at which an accident will occur against vehicle speed and wind direction. The current methodology direct that this procedure should be carried out for different degrees of unbalanced lateral accelerations – effectively simulating the passage of trains around curves with either cant deficiency or cant excess i.e. where the centrifugal forces are not balanced by the train weight component due to the cant, or camber, of the track, and where there is thus a lateral force on the track. In vehicle authorisation the CWCs thus derived are compared with standard reference values for each class of train, although such curves are only currently given for high speed Class 1 trains. In the assessment of route risk, the accident wind speeds are used in conjunction with meteorological information of wind conditions along the route to determine the risk of an overturning accident occurring.

https://doi.org/10.1017/S0001924000009179 Published online by Cambridge University Press

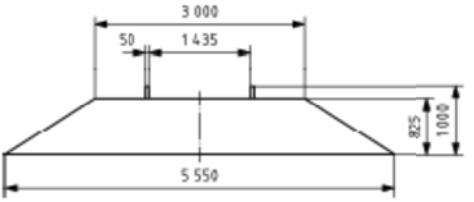

Figure 19. The single track ballasted rail simulation for wind tunnel tests[8].

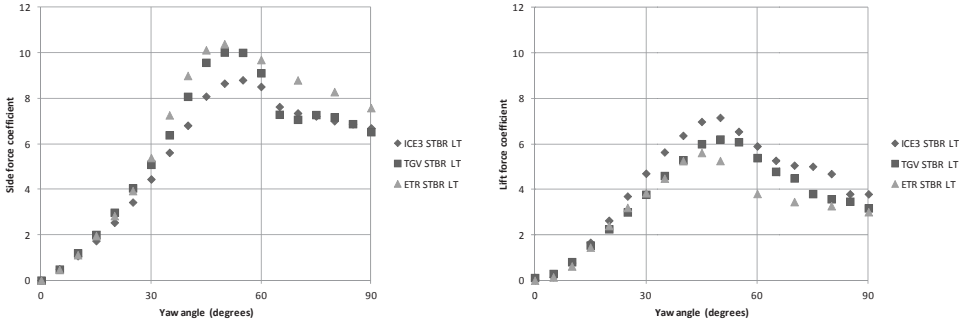

Figure 20. Side and lift force coefficients for Class 1 trains[8] (The *x* axis shows the yaw angle, and the *y* axis the side force and lift force coefficient values).

Now in a recent paper[54] the author has argued that the current methodology is overly complex and the complexity of the central part of the methodology (the calculation of the cross wind characteristics) is inconsistent with the very large uncertainties inherent in the specification of the aerodynamic characteristics and the route exposure. In addition, as argued above in relation to a number of other issues, applying limit values (in this case reference CWCs) to the results of calculations based on vehicle characteristic alone does not really address the issues that require addressing, which is the specification of the risk of an accident. In that paper the author proposes a simplified methodology which can be applied consistently in the train authorisation and route risk assessment procedure with a balance of uncertainties throughout the process. The arguments of that paper will not be repeated here, where we will rather dwell on more fundamental matters and issues arising from the current CEN methodology.

6.3 Aerodynamic characteristics

When trains are subject to a cross wind they experience three aerodynamic forces (drag, side and lift forces along the *x, y* and *z* axes respectively) and three aerodynamic moments (roll about the *x* axis, pitch about the *y* axis and yaw about the *z* axis). Data for such forces and moments can be obtained from either wind-tunnel tests or from CFD calculations. In either of these there are modelling choices to be made. The simplest wind tunnel or CFD simulation would be to use a stationary model mounted on some sort of representation of the track, with the effect of different wind directions modelled by turning the model at different angles to the oncoming flow. Such a simulation neglects both the effects of atmospheric turbulence and shear and the effects of vehicle movement relative to the ground. Nonetheless simulations of this type are in common use, and are quite valid for high speed trains, where atmospheric turbulence levels are small in comparison to the train speed and the train actually 'sees' a basically steady flow wind at a small yaw angle – see Part 1. In the past a number of standard ground simulations have been used – flat ground, single

https://doi.org/10.1017/S0001924000009179 Published online by Cambridge University Press

and double ballasted track representations etc. The standard simulation that has been adopted by CEN is the 'single track ballasted rail' or STBR, which is shown in Fig. 19[8]. For low speed or stationary vehicles however it is necessary to model the atmospheric turbulence and shear using the standard methodology adopted in atmospheric boundary-layer wind tunnels. Again this is an approximation that while absolutely valid for stationary vehicles, becomes less so as the vehicle speed increases. Finally experiments or simulations can be made with a vehicle moving across the ground. Experimentally this is very complex and has not often been attempted –see Ref. 55 for example. In CFD terms it is somewhat easier to achieve such a simulation by moving the floor of the computational domain. In the first instance we will consider the side and lift force characteristics only. Figure 20 shows the variation of these forces for the ETR500, TGV Duplex and the ICE3 train, from the data given in Ref. 8, expressed in terms of side and lift force coefficients, with the forces normalised by $0{\cdot}5\rho AV^2$, where ρ is the density of air, A is a reference area (conventionally taken as $10m^2$) and V is the air velocity relative to the train (ie the vector sum of the wind and vehicle velocities). The coefficients are plotted against yaw angle. These coefficients were obtained from low turbulence wind-tunnel tests, with the standard ground configuration. It can be seen that at low yaw angles both side and lift force coefficients increase with yaw angle, before levelling off and decreasing at higher yaw angles. These two regions correspond to the two flow regions described in Part 1, with the yaw angle range between about 40 and 70° being a transition region between them. In recent decades measurements have been made of a wide variety of different train types, and this form seems quite general, although the fall off at high yaw angles is not always apparent.

However, in the overturning situation, the most important parameter is the rolling moment coefficient about the leeward rail (i.e. the point of tipping). This is a combination of the moments due to the side force and the lift force and the (small) rolling moment about the x axis through the vehicle centre. In two recent papers[54,56] the author has analysed a large data set of side force, lift force and lee rail rolling moment coefficients and showed that if they are normalised by their value at 40°, then at least in the low yaw angle range (which is actually the range of practical importance for high speed trains) the data collapses onto a single curve for different categories of train, that is easily parameterised. Results for the lee rail rolling moment coefficient are shown in Fig. 21 for high speed very streamlined trains, less streamline trains, blunt trains and for trailing vehicles[56]. In the lower yaw angle range, these curves can be parameterised by curves of the form

$$\frac{C_{RL}(\psi)}{C_{RL}(40)} = \left(\frac{\mathrm{Sin}(\psi)}{\mathrm{Sin}(40)} \right)^n \quad \ldots (10)$$

where $n = 1{\cdot}6$ for streamlined passenger trains, $1{\cdot}2$ for non-streamlined leading vehicles and $1{\cdot}7$ for trailing vehicles. Table 4 shows a collation of the values of lee rail rolling moment coefficient at 40 degrees for the ETR500, TGV and ICE3 trains from the CEN code [8]. One interesting point is that different types of wind-tunnel test for the same train can produce quite a wide range of different values of the coefficient at 40 degrees. Specifying n and the value of the rolling moment coefficient at 40 degrees thus gives an extremely convenient way of categorising train rolling moment characteristics that has proved useful in developing the methodology of Ref. 54.

In addition to the experimental results mentioned above and used in the compilation of Fig. 21, there are a range of other reports of similar work and equivalent CFD calculations in the literature – see for example CFD calculations on generic train shapes[63]; wind-tunnel measurements on freight trains[64]; CFD and wind-tunnel measurements on high speed trains[65-67]; and wind-tunnel measurements and CFD calculations of a variety of passenger trains on bridges, viaducts and

https://doi.org/10.1017/S0001924000009179 Published online by Cambridge University Press

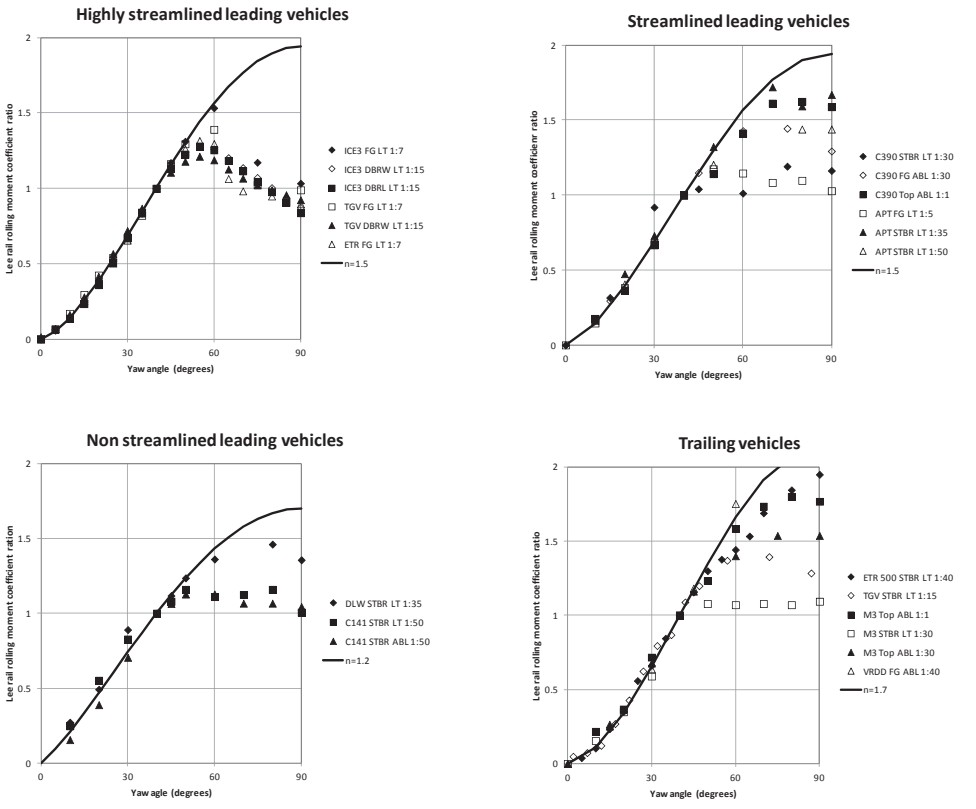

Figure 21. Parameterisation of lee rail rolling moment coefficients (Sources for data are given in Ref. 56. Legend indicates train type (ICE – German high speed train[8]; TGV – French high speed train [8,57]); ETR – Italian high speed train[8,58]; C390 – GB Class 390[59,60]; APT – GB Advanced Passenger Train (61); DLW – GB Derby Lightweight[61]; C141 – GB Class 141 multiple unit[61]; M3 – GB Mark 3 coach[59,60]; VRDD – Finish railways double deck coach[62]), ground simulation (STBR – single track ballasted rail; DBRW – double ballasted rail leeward; DBRL – double ballasted rail leeward; FG – flat ground; Top – topography representation), wind simulation (LT – low turbulence; ABL – Atmospheric boundary layer) and scale).

embankments[58,68-70]. The latter are particularly important for route risk calculations where different types of infrastructure need to be considered.

6.4 Overturning calculations, gusts and CWC

The next stage in the process of calculating CWCs is to use a model of the vehicle wind system. As noted above this can have varying degrees of complexity. The simplest is the three mass model which allows for some representation of the sprung and unsprung masses and makes some simple allowance for suspension effects. The wind gust in such calculations is implicitly a maximum gust value. Different levels of complexity have been used by other authors – five mass models and MBS levels with varying numbers of degrees of freedom. The more complex method use all six force and moment components. The wind field applied to these models also differs in complexity. The preferred method in the current CEN code[8] is to use the Chinese Hat gust as a representation of a real gust – Fig. 22. The author has considerable misgivings concerning this. The Chinese Hat gust seems to have been developed in wind loading studies for wind turbines as a time dependent

https://doi.org/10.1017/S0001924000009179 Published online by Cambridge University Press

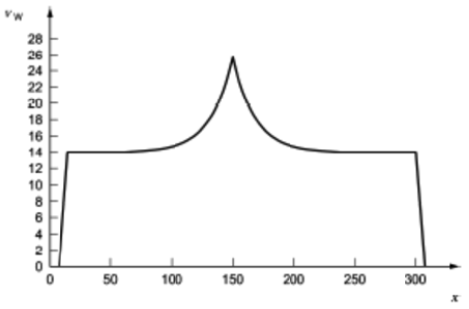

Figure 22. Chinese Hat wind gust.simulation[8].

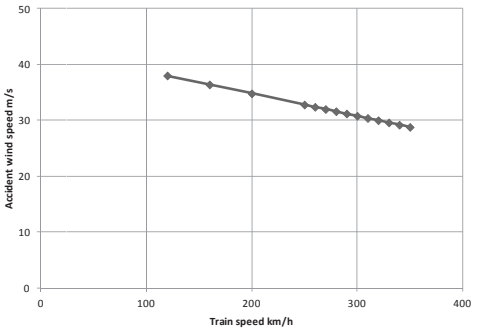

Figure 23. Cross wind characteristic for Class 1 vehicle using Chinese Hat simulation[8].

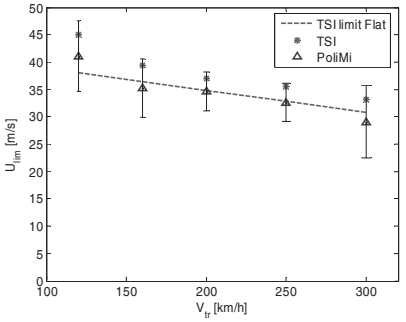

Figure 24. cross wind characteristic using full simulation of wind turbulence[52].

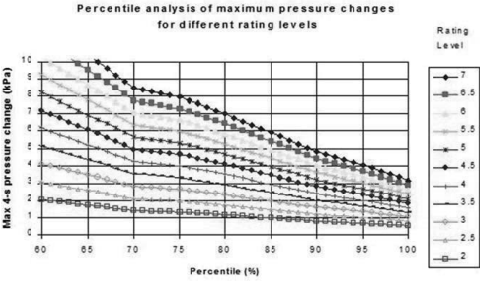

Figure 25. Subjective response of humans to pressure transients[74] (The *x* axis shows the percentile of the population, who experience the maximum 4 second pressure transient on the *y* axis at a particular comfort level. These range from 1 – no discomfort, to 7 – painful).

gust based upon the temporal correlations of the gust statistics passing a point (as specified by the wind speed correlation functions[71]. For such a situation this is an appropriate method. However, in its use in the code, this has been transformed into a spatially varying gust through which the train passes, with the temporal characteristics being replaced by spatial characteristics through the spatial wind correlations, in a one to one fashion. This is not theoretically sound and the present author can see no justification for this approach. Ideally some sort of gust varying both spatially and temporally is required. Finally the most complex gust formulation is to generate the complete stochastic wind field as seen by the train as in Ref. 52. These investigators coupled this with the

Table 4
Lee rail rolling moments at 40 degrees yaw for different ground configurations for Class 1 trains[8]

	Flat Ground	Single track ballasted rail	Double track ballasted rail windward side	Double track ballasted rail leeward side
ICE3	4·57	5·36	4·86	5·05
TGV Duplex	5·13	6·10	5·15	5·74
ETR500	5·84	7·14		

https://doi.org/10.1017/S0001924000009179 Published online by Cambridge University Press

specification of an aerodynamic admittance that allows for the non-correlation of turbulence over the side of the train. Whatever the approach used, CWCs of the form shown in Fig. 23 for the reference Class 1 vehicle in the Rolling Stock TSI can be obtained. This, as would be expected, shows a fall off in the wind speed required for an accident to occur as the vehicle speed increases. A similar curve is shown in Fig. 24 which shows a similar curve for the ETR 500, but calculated over a large number of realisations of a full stochastic approach, using simulated wind time series. It can be seen that there is considerable variation of the curve about the mean value[52].

As has been mentioned above, in a recent paper the author has proposed a greatly simplified methodology[54]. In this methodology the simple rolling moment correlations outlined above are used, which allows the definition of parameter he describes as the characteristic wind speed, defined as:

$$c^2 = \frac{\gamma Mg\theta(\mathrm{Sin}(40))^n}{0\cdot 5\rho C_{RL}(40)Ah} \qquad \ldots (11)$$

where γ is a parameter that allows for suspension effects and a range of other 'real' effects and θ is the track semi-width. This in turn is used, with a simple vehicle analysis, to generate generic and easily parameterised cross wind characteristics than can be generally applied. This generic cross wind characteristic is given by:

$$\left(\frac{u_i}{c}\right) = 1 + a_1\left(\frac{v}{c}\right) + a_2\left(\frac{v}{c}\right)^2 + a_3\left(\frac{v}{c}\right)^3 + a_4\left(\frac{v}{c}\right)^4 \qquad \ldots (12)$$

where u_i is the wind speed for an incident to occur and:

$$a_1 = -1\cdot 0539 + 1\cdot 2885n - 0\cdot 4059n^2 \quad , a_2 = 0\cdot 071 - 0\cdot 5584n + 0\cdot 2873n^2,$$
$$a_3 = 0\cdot 0484 + 0\cdot 1528n - 0\cdot 0993n^2, \quad a_4 = -0\cdot 0042 - 0\cdot 025n + 0\cdot 01529n^2 \qquad \ldots (13)$$

The simplified vehicle mode has been calibrated against a more complex approach and can include first order corrections for real effects, such as suspension effects, admittance effects and track irregularities.

6.5 Risk analysis

However they are derived the cross wind characteristics can then be used, together with meteorological data to find the probability that, at a particular section of track the wind speed will exceed the accident wind speed and an overturning incident will occur. A number of such methods (those used in Germany, France, Italy and the UK) were considered during the AOA project during which a comparative exercise was carried out[72]. A detailed comparison is not given here, but as well as varying in the manner in which cross wind characteristics are derived, these methods also vary in the way in which meteorological conditions are derived and assessed, with some methods using existing wind data, modified for local effect by terrain factors such as those found in wind loading codes of practice, whist others use large scale CFD modelling of the orography around the route. The nature of the wind speed probability distributions, and the convolution of these distributions with the CWCs also takes on a number of forms.

The probability of the local wind speed exceeding the accident wind speed having been obtained, there are also considerable differences in how this information is used and interpreted. Some methods take into account train operations – how often and for how long trains will be

https://doi.org/10.1017/S0001924000009179 Published online by Cambridge University Press

in a particular section of route, the consequences of an accident, potential number of fatalities etc., while others simply focus on the train itself. The resulting risks are then considered either by comparing the risk with the risk of an accident on existing operations that are perceived to be safe, or by calculating an absolute risk level, and can be used to inform the construction of wind protection along the track or the development of traffic restriction strategies during strong winds.

Whatever the precise methodology that is used, it is found that the final risk value is firstly very sensitive to small changes in the input parameters, and can only really be specified to the nearest order of magnitude, and secondly, a very large proportion for the risk comes from just a few exposed sites on any particular route.

The simplified methodology of (54) describes above allows for such a risk analysis to be carried out. For a particular section of track the overall risk of a fatality can be shown to be

$$\Omega = e^{-\left(\frac{u_i}{\lambda}\right)^k} f\left(\frac{v}{v_r}\right)^m \left(\frac{SN}{3600v}\right) \quad \ldots (14)$$

Here λ and k are the parameters of the Weibull distribution for gust wind speeds, which are a function of the mean wind speed values and the turbulence intensity; u_i is the wind speed at which an accident will take place (Equation (12)), f is a constant, giving the risk of a fatality) at a reference speed v_r, v is the vehicle speed, m is an exponent of order 4 to 8, S is the length of the section and N is the number of services on the section each hour. This parameter can be directly used in the process of vehicle certification, with specified reference values of the Weibull parameters. For a route risk analysis, the risk should be calculated for each section of track and the total risk / year obtained from the sum of the section risks.

7.0 PRESSURE TRANSIENTS IN AND AROUND TUNNELS

7.1 Passenger comfort

Within the design process, the aural comfort of passengers is taken into account through the imposition of pressure transient limits. These are in general based on work that was carried out in the 1980s that looked at the response of individuals to imposed pressure time series, often through the use of pressure chamber tests[73] and through physiological considerations. Clearly the nature of the pressure transients will change between the case of sealed trains and unsealed trains. Most modern high speed trains would be sealed, and the internal pressure will lag the external pressure quite considerably. The degree of sealing is specified by a leakage time constant, with the value of this parameter for unsealed trains being less than 0·5s. There is a reasonable degree of agreement on appropriate pressure transient limits and those given in CEN[7] are as follows for unsealed and sealed trains,

For unsealed trains

- 4·5kPa within a period of 4s for the worst case of two trains passing in a double tack tunnel.
- 3·0kPa within a period of 4s for a single track tunnel.

For sealed trains (with a leakage time constant of greater than 0·5s) for both single and double track tunnels

- 1·0kPa within a period of 1s
- 1·6kPa within a period of 4s
- 2·0kPa within a period of 10s

https://doi.org/10.1017/S0001924000009179 Published online by Cambridge University Press

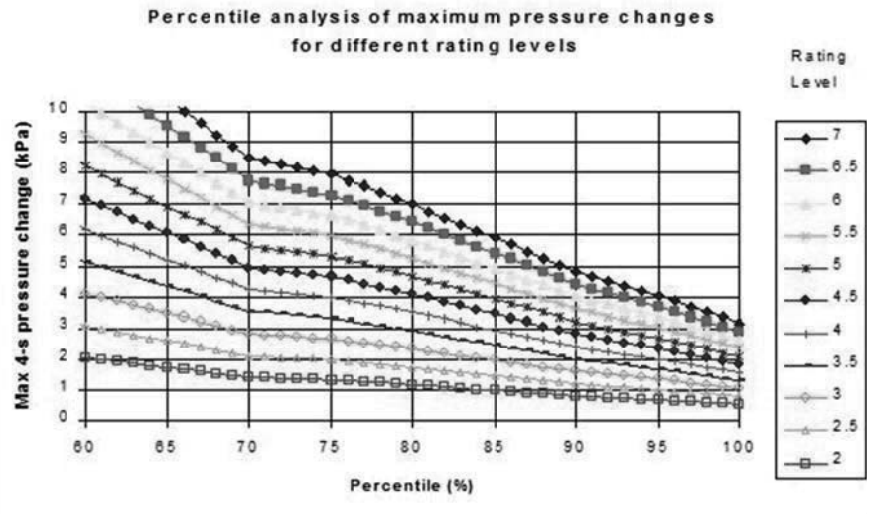

Figure 25. Subjective response of humans to pressure transients[74] (The *x* axis shows the percentile of the population, who experience the maximum 4 second pressure transient on the *y* axis at a particular comfort level. These range from 1 - no discomfort, to 7 – painful).

For the unsealed train, the differences between the criteria for single and double track tunnels are due to the fact that the double track criterion is for the worst case, while the single track criterion will be repeated for each train pass. For sealed trains, the longer term pressure differences become to be more of an issue.

It should be noted that these are essentially deterministic criteria, with the variability of human response allowed for by choosing upper limits of acceptable pressure transients. Another possible methodology would be to carry out an analysis similar to that adopted for the calculation of the risk of slipstream accidents, based on curves such as those shown in Fig. 25 (from Ref. 74, based on the results of Ref. 73 which show the cumulative probability of human response for pressure transients of different levels, with different comfort criteria. For a double track tunnel the procedure would be as follows.

- Assume that the probability distribution of the maximum pressure transients, p, in a tunnel, for the complete range of train crossing points, is given by a normal distribution of mean m_p and standard deviation s_p. These values can be obtained using multiple runs of standard analysis software for predicting pressure transients in tunnels.
- Assume that the cumulative probability distributions for human response in Fig. 25 can be given by:

$$\begin{aligned} \mu_r &= 0 \text{ for } p < a \\ \mu_r &= (p-a)/b \text{ for } a < p < a+b \\ \mu_r &= 1 \text{ for } a+b < p \end{aligned} \qquad \ldots (15)$$

From Fig. 25, a and b can be taken to be given by:

$$a = 0{\cdot}51R\text{-}0{\cdot}43 \qquad b = 3{\cdot}13R\text{-}3{\cdot}52 \qquad \ldots (16)$$

where R is the pressure comfort rating.

- The probability that two trains will actually meet in the tunnel is given by:

https://doi.org/10.1017/S0001924000009179 Published online by Cambridge University Press

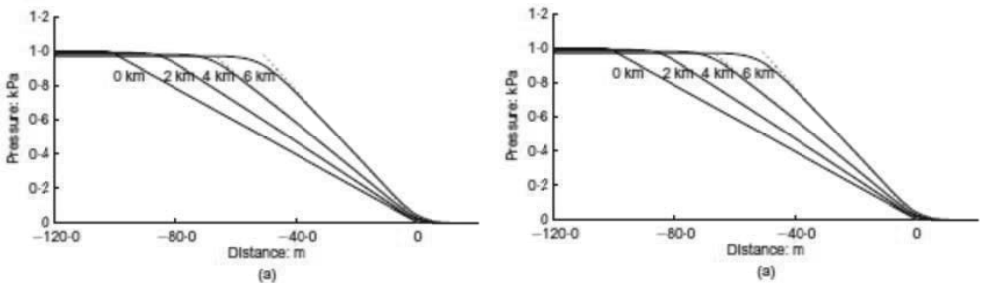

Figure 26. Pressure gradient steepening in ballasted track tunnels (top) and slab track tunnels (bottom)[75].

$$\mu_D = \left[\frac{\left(\frac{T}{v}\right)}{60 s_D \sqrt{2\pi}} e^{-\frac{1}{2}\left(\frac{\Delta}{s_D}\right)^2} \right] \quad \ldots (17)$$

where T is the length of the tunnel and v is the train speed, Δ is the timetabled time between the two trains entering the tunnel, and s_D is the standard deviation of the delay of any one train from the timetabled arrival time.

- The risk that a specific comfort rating will be exceeded by any one passenger on any one train pass through the tunnel is then given by:

$$\Omega = \left[\frac{\frac{L}{v}}{60\sigma_D\sqrt{2\pi}} e^{-\frac{1}{2}\left(\frac{\Delta}{\sigma D}\right)^2} \left(0{\cdot}5(1-erf(\beta)) + \frac{1}{\beta-\alpha}\left(\frac{1}{\sqrt{\pi}}\left(e^{-\alpha^2} - e^{-\beta^2}\right) + \frac{\alpha}{2}\left(erf(\alpha) - erf(\beta)\right)\right)\right)\right] \quad \ldots (18)$$

where:

$$\alpha = \frac{a - m_s}{\sqrt{2s_s}} \qquad \beta = \frac{a + b - m_s}{\sqrt{2s_s}} \quad \ldots (19)$$

This method can be directly used in the consideration of the design and operation of a specific tunnel, and overall route risk can be determined by summing the risk for individual tunnels along the route.

7.2 Micro pressure waves

The existence of micro-pressure waves, or sonic booms, at the exit to tunnels has already been mentioned in Part 1. Essentially these form because of the steepening of the initial pressure wave as it passes along the tunnel, and when it is reflected at the tunnel exit, some pressure fluctuations, of a considerably lower magnitude than those that pass up and down the tunnels, are radiated out from the tunnel outlet. This effect is most noticeable in long tunnels, where the pressure waves have a greater distance of travel in which to steepen, and for slab track (concrete) tunnels rather than ballasted tunnels, since the frictional damping of the pressure waves in the former is much lower than in the latter. The steepening is due to the faster speed at which the back of the wave front moves in comparison to the front of the wave front. This phenomenon is very well

https://doi.org/10.1017/S0001924000009179 Published online by Cambridge University Press

Figure 27. Construction of sonic boom alleviation section on the Finnetunnel tunnel in Germany[76].

described in detail in Ref. 75. That paper describes methods for calculating whether or not such micro-pressure waves will occur, and if they do occur, methods for their alleviation. The former is straightforward at least in principle. Firstly the magnitude and gradient of the initial pressure rise can be calculated, either from standard formulae, from experiments, or from CFD calculations. These will be functions of tunnel blockage ratio and train speed. For short tunnels, these values of magnitude and gradient can be assumed to exist at the outlet of the tunnel as well as at the inlet. However, for long tunnels the steepening of the wave along the length of the tunnel must be calculated – see Fig. 26. This is straightforward for slab track tunnels, but much less so for ballasted tunnels where reliable methods do not exist. However this is of little practical importance, as there are usually no problems with micro-pressure waves in ballasted tunnels. At the exit, acoustic theory can then be used to calculate the magnitude and frequency of the external micro-pressure waves.

In order to reduce these magnitudes the methods that are normally adopted are to modify the tunnel entrance, through the introduction of an area of decreasing cross section. This reduces the gradient of the initial pressure wave, and thus of the emitted micro-pressure waves. A typical construction – on the Finnetunnel tunnel in Germany – is shown in Fig. 27[76]. The pressure gradients can also be reduced by the lengthening of train noses as in recent versions of the Shinkansen train trains. The exit pressure gradients can also be modified by modifications along the tunnel – airshafts, refuges, and perhaps ballast modifications. Surprisingly modifications to the tunnel exit, such as ventilated exit regions have not been found to be effectives. Reference 75 also describes a number of attempts to use active devices – such as ‘anti-noise’ generation, and the release of large quantities of air to disrupt the pressure rise in any passing wave. These have been shown to be effective, but suffer from the problem associated with all such active devices of lack of reliability during power outages etc.

This leaves the issue of what are the acceptable levels of radiated pressure at the tunnel exit. This issue has been considered in Ref. 77. The authors of that paper studied the entire process

https://doi.org/10.1017/S0001924000009179 Published online by Cambridge University Press

of entry wave steepening and radiation from the end of the tunnel, showing that the wave steepening calculations worked well, but the uncertainty in the solid angle over which the sound radiated outside the tunnel was large. Criteria for maximum sound levels were derived from an EU directive for *C* weighted sound levels. They suggest that within 25m of the exit from a tunnel tunnel, these levels should not exceed 115 dB(C) while the levels at the nearest properties should not exceed 75 dB(C).

8.0 OTHER ISSUES

The preceding sections have outlined a range of railway aerodynamic issues that are of major current relevance. But they are by no means the only aerodynamic issues that exist that may be of importance in some circumstances. In Part 1 the scope of this paper was deliberately stated to exclude the subject of aero-acoustics. Acoustic issues, arising from both mechanical and aerodynamic effects, however, can be of major concern in the development of new trains and infrastructure as it directly impinges upon those who live in the vicinity of railway lines. Further details of current work in this area can be found in Ref. 78. Similarly the scope of this paper was deliberately limited to exclude MagLev vehicles. While there has been some recent MagLev developments, most notably in Germany[79] and China[80] this mode of transport has perhaps not lived up to its early promise. However the current plans for the ultimate replacement of the Japanese Shinkansen fleet by MagLev systems may result in the need for further work in this area. More details of the aerodynamics of Maglev systems can be found in Ref. 2.
Some other issues that are of importance include.

- The movement of airborne particles of all sizes in the vicinity of the railway line – microscopic heavy metal particles from track and brake wear that may have health effects[81]; dust movement, particularly in tunnels, again with health and soiling implications[82]; and the blowing of coal/rock dust from open wagons[83].
- The relative movement between pantographs and the overhead wire system in high cross winds, which can in extreme cases result in the phenomenon known as ‘dewirement’ where the wire is trapped beneath the pantograph head, with resulting major damage. A discussion of this phenomenon is given in Ref. 84. In the UK, there is a system of vehicle speed restrictions in place in high wind speed conditions.
- Recently a number of authors have reported on the effect of cross winds on trains on long span bridges where coupled calculations have been carried out considering bridge and train aerodynamics and dynamics, and the coupling of these different effects, in order to understand the effect of trains on bridge stability in cross winds, and bridge movement on the stability of trains in cross winds[85,86].
- Some work has been carried out to consider the loads on trains in very sudden gusts such as downburst and tornadoes, and in particular considered the overshoot of the cross wind forces above the mean values during the establishment of the flow[87].
- As noted in Section 6 above there a number of other cross wind issues that are of concern, in particular wind effects on track lateral load and gauge infringement. The interested reader should refer to Refs 46 and 47 for further details.
- In recent projects, some concern has been expressed as to the effect of new trains on birds or small animals, either through direct collision with trains, or through major disturbance caused by the train slipstream. This problem can in principle be addressed using the methodology

https://doi.org/10.1017/S0001924000009179 Published online by Cambridge University Press

briefly described in Section 5 for predicting the flight of ballast, although to predict the animal movement in train slipstreams, some realisation of unsteady wind fields is required, either through moving model experiments, or through unsteady CFD simulations.

9.0 CONCLUDING REMARKS

It can be seen from the material presented in earlier sections that the range of train aerodynamic problems is extremely diverse, and the range of methodologies required to address these problems is equally diverse. Perhaps the major point to emerge, and the one which the writer would wish to emphasise, is the essentially ad hoc nature in which may of the problems have been addressed, design limits specified etc. Often the nature of the flow field around the train that causes these problems is not fully considered and, more importantly, the limits are related to parameters that can easily be measured, rather than those that are actually of concern to the passenger or train operator. It would seem to the author that a much better approach would be to consider all these issues within a consistent risk analysis framework, that allocates risk levels to different issues that are consistent with the risks arising from other aspects of train operation, and to use these risks as design targets. This would allow a proper appreciation of aerodynamic risk in comparison to that from other sources. Whist such an approach has been adopted for certain aerodynamic effects in certain railway administrations, it is very far from universal. This issue has been addressed to some extent in this paper, but there is scope for much more work and development in this area.

ACKNOWLEDGEMENTS

It will be evident from the reference list that the author is indebted to a large number of industrial and academic colleagues and research students past and present for much of the information that is included in this paper, and it is simply not possible to name them all. Their contribution is gratefully acknowledged. However, the author would specifically like to acknowledge the part played by Roger Gawthorpe, former Head of Aerodynamics Research at British Rail, and the one who first introduced him to the fascinating subject of train aerodynamics.

Figures from other sources

The author would like to acknowledge the permissions given by various organisations and individuals to reproduce figures for this paper. These are as follows. Figs 1 and 17 Reproduced with permission from WCRR; Figs 19, 22 Permission to reproduce extracts from British Standards is granted by BSI Standards Limited (B BSI); Figs 2, 3, 7, 9, 16 Reproduced with permission from Sage Publications Ltd; Fig. 4 Reproduced with permission from the author; Fig. 10 Reproduced with permission from the authors; Fig. 11 Permission granted by Elsevier under license number 3258160523011; Figs 12 and 13 Reproduced with permission from the authors; Fig. 14 Reproduced under the Creative Commons License held by TU Berlin; Fig. 24 Reproduced with permission from the authors; Fig. 25 Presented and published at BHR Group's 10th International Symposium on Aerodynamics and Ventilation of Vehicle Tunnels, Boston, USA. Reproduced with permission; Fig. 26 Published with permission from ICE publishing under license number 3292001037426; Fig. 27 Reproduced with permission from the authors

REFERENCES

1. GAWTHORPE, R.G. Aerodynamics of trains in the open air, *Railway Engineer International,* 1978, **3**, (3), pp 7-12.
2. SCHETZ, J.A. Aerodynamics of high speed trains, *Annual Review of Fluid Mechanics*, 2001, **33**, pp 371-414.
3. RAGHUNATHAN, R.S., KIM H.D. and SETOGUCHI, T. Aerodynamics of high speed railway train, *Progress in Aerospace sciences*, 2002, **38**, (6–7), pp 469–514.
4. CEN (2003), Railway Applications – Aerodynamics Part 2 Aerodynamics on Open Track E BS EN 14067-2:2003.
5. CEN (2003) Railway Applications – Aerodynamics Part 3 Aerodynamics in tunnels BS EN 14067-3:2003.
6. CEN (2009) Railway Applications – Aerodynamics Part 4 Requirements and test procedures for aerodynamics on open track, BS EN 14067-4:2005+A1:2009.
7. CEN (2010) Railway Applications – Aerodynamics Requirements and test procedures for aerodynamics in tunnels, BS EN 14067-5: 2006+A1:2010.
8. CEN (2010) 'Railway Applications – Aerodynamics'. Aerodynamics Tests for crosswind assessment, BS EN 14067-6:2010.
9. TSI (2008) 'EU Technical Specification for Interoperability Relating to the 'Rolling Stock' Sub-System of the Trans-European High-Speed Rail System' HS RST TSI, 2008/232/EC.
10. TSI (2008) 'EU Technical Specification for Interoperability Relating to the 'Infrastructure Sub-System of the Trans-European High-Speed Rail System' HS RST TSI, 2008/217/EC.
11. ROCHARD, B.P. and SCHMID, F. A review of methods to measure and calculate train resistances, Proceedings of the Institution of Mechanical Engineers, *Part F: J Rail and Rapid Transit*, 2000, **214**, pp 185-199.
12. BROCKIE, N.J.W. and BAKER, C.J. The aerodynamic drag of high speed trains, *J Wind Engineering and Industrial Aerodynamics*, 1990, **34**, pp 273-290.
13. GUIHEU, C. Resistance to forward movement of TGV-PSE trainsets: evaluation of studies and results of measurements, *French Railway Review,* 1983, **1**, (1), pp 13–26.
14. HUANG, S., LI, Z., YANG, M. and CHEN, Z. Research on the Moving Model Measuring Method of High-speed Train Aerodynamic Drag Based on Machine Vision, Proceedings of the International Workshop on Train Aerodynamics, 2013, Birmingham, UK.
15. MANCINI, G., MALFATTI, A., VIOLI, A.G. and MATSCHKE, G. Effects of experimental bogie fairings on the aerodynamic drag of the ETR 500 high speed train, World Congress on Railway Research, 2001, Munich, Germany.
16. HEINE, C. and MATSCHKE, G. The influence of nose shape on high speed trains on the aerodynamic coefficients, Koln, Germany.
17. WATKINS, S., SAUNDERS J.W. and KUMAR, H. Aerodynamic drag reduction of goods trains, *J of Wind Engineering and Industrial Aerodynamics*, 1992, **40**, (2), pp 147–178.
18. KRAJNOVIC, S. Shape optimization of high-speed trains for improved aerodynamic performance, Proceedings of the Institution of Mechanical Engineers, *Part F: J Rail and Rapid Transit*, 2009, 223, 439, 10.1243/09544097JRRT251.
19. TIAN, H. Formation mechanism of aerodynamic drag of high-speed train and some reduction measures, *J the Central South University of Technology*, 2009, **16**, 0166−0171.
20. BEAGLES, A.E. and FLETCHER, D.I. The aerodynamics of freight; approaches to save fuel by optimising the utilisation of container trains, Proceedings of the RRUK-A Annual Conference, 2012, London.
21. MAEDA, T., KINOSHITA, M., KAJIYAMA, H. and TANEMOTO, K. Estimation of aerodynamic resistance of Shinkansen trains from pressure rise in tunnel, Proceedings of the 6th International Symposium on Aerodynamics and Ventilation of Vehicle Tunnels, 1988, Durham, UK.
22. LUKASZEWICZ, P. Energy consumption and running time for trains, 2001, PhD Thesis, KTH, Sweden.
23. ARMSTRONG, D.S. and SWIFT P.H. Lower energy technology, Part A Identification of energy use in multiple units, Report MR VS 077, 1990, British Rail Research, Derby, UK.
24. KUMAR, A., RICKETT, T.G., VEMULA, A., HART, J.M., EDWARDS, J.R., AHUJA, N. and BARKAN, C. Aerodynamic Analysis of Intermodal Freight Trains Using Machine Vision, Proceedings of the World Congress on Railway Research, 2011, Lille, France.
25. VARDY, A.E. Aerodynamic drag on trains in tunnels Part 1: synthesis and definitions, Proceedings of the Institution of Mechanical Engineers, 1996, *Part F: J Rail and Rapid Transit,* 1996, **210**, (29), 10.1243/PIME_PROC_1996_210_324_02, Part 2: prediction and validation, Proceedings of the Institution of Mechanical Engineers, Part F: J Rail and Rapid Transit 1996 210, 39, 10.1243/PIME_PROC_1996_210_325_02.

26. SOCKEL, H. Formulae for the Calculation of Pressure Effects in Railway Tunnels, Proceedings of the 11th International Symposium on Aerodynamics and Ventilation of Vehicle Tunnels, Luzern, Switzerland, 2003, **2**, (581).
27. BAKER, C.J., JORDAN, S.J., GILBERT, T., STERLING, M., QUINN, A., JOHNSON, T. and LANE, J. Transient aerodynamic pressures and forces on trackside and overhead structures due to passing trains. Part 1 Model scale experiments, 2012, *J Rail and Rapid Transit*, 10.1177/0954409712464859.
28. SANZ-ANDRES A., LAVERON, CUERVA, A. and BAKER, C. Vehicle-induced loads on pedestrian barriers, *J Wind Engineering and Industrial Aerodynamics*, 2004, 92,403-426, 10.1016/j.jweia.2003.12.004.
29. JOHNSON, T. and DALLEY, S. 1/25 scale moving model tests for the TRANSAERO Project. in TRANSAERO – A European Initiative on Transient Aerodynamics for Railway System Optimisation. 123-135, Notes on Numerical Fluid Mechanics and Multidisciplinary Design, 2002, **79**, SCHULTE-WERNING, B., GREGOIRE, R., MALFATTI, A. and MATSCHKE, G. (Eds).
30. RSSB Review of slipstream effects on platforms, Report prepared for the Rail Safety and Standards Board by J Temple and T Johnson of AEA Technology Limited for project T248, 2003.
31. BAKER, C.J., QUINN, A., SIMA, M., HOEFENER, L. and LICCIARDELLO, R. Full-scale measurement and analysis of train slipstreams and wakes. Part 2 Gust analysis, Proceedings of the Institution of Mechanical Engineers, *Part F: J Rail and Rapid Transit*, 2013, 0954409713488098.
32. BAKER, C.J., GILBERT, T. and JORDAN, S. The validation of the use of moving model experiments for the measurement of train aerodynamic parameters in the open air, Proceedings of the World Congress on Rail Research, 2013, Sydney, Australia.
33. RAPIDE Railway aerodynamics of passing interaction with dynamic effects. Synthesis report, Aerodynamics Workshop, 2001, Cologne.
34. JORDAN, S.C., JOHNSON, T., STERLING, M. and BAKER, C.J. Evaluating and modelling the response of an individual to a sudden change in wind speed, *Building and Environment*, 2008, **43**, pp 1521-1534, 10.1016/j.buildenv.2007.08.004.
35. BAKER, C.J. Risk analysis of pedestrian and vehicle safety in windy environments, IN-VENTO Italian Society for Wind Engineering, 2014, Genoa, Italy.
36. KALTENBACH, H.-J. DeuFraKo Project – Aerodynamics in Open Air (AOA) WP 1 Underfloor Aerodynamics Summary Report.
37. SHINOJIMA, K. Study on the phenomena of snow adhering to and dropping from shinkansen train, and the countermeasures, *Quarterly Reports*, 1984, **25**, (2), pp 41-44.
38. QUINN, A.D., HAYWARD, M., BAKER, C.J., SCHMID, F., PRIEST, J.A. and POWRIE, W. A full-scale experimental and modelling study of ballast flight under high-speed trains, Proceedings of the Institution of Mechanical Engineers, Part F: J Rail and Rapid Transit, 2010, **224**, (2), pp 61-74, 10.1243/09544097JRRT294.
39. SAUSSINE, G., MASSON, E., JAQUES, T.-J., PARADOT, N., ALLAIN, E. and JOSSE, F. Railway Ballast flying phenomena – from numerical simulation towards risk assessment, EUROMECH Colloquim 509, Vehicle Aerodynamics, External aerodynamics of railway vehicles, trucks, buses and cars, 2009, Berlin, Germany.
40. KALTENBACH, H.-J, GAUTIER, P.-E., AGIRRE, G., ORELLANO, A., SCHROEDER-BODENSTEIN, K., TESTA, M. and TIELKES, Th Assessment of the aerodynamic loads on the trackbed causing ballast projection: results from the DEUFRAKO project Aerodynamics in Open Air (AOA), Proceedings of the World Congress on Rail Research, 2008, Seoul, South Korea, Paper number S2.3.4.1.
41. SAUSSINE, G., ALLAIN, E., VAILLANT, A., RIBOURG, M. and NÉEL, O. High speed in extreme conditions: ballast projection phenomenon, Proceedings of the International Workshop on Train Aerodynamics, 2013, Birmingham, UK.
42. Railway Archive, Furness Railway http://www.railwaysarchive.co.uk/documents/BoT_LevenViaduct1903.pdf, 2013.
43. EAST, J.R. 2006, Current Measures in Response to the Uetsu Line Accident, http://www.jreast.co.jp/e/press/20060101/ Accessed 04/08/2013.
44. Xinhua News Agency (2007) Strong Wind Derails Train, Killing 4 http://www.china.org.cn/english/China/200975.htm, Accessed 04/08/2013.
45. WETZEL, C. and PROPPE, C. Crosswind stability of high speed trains; a stochastic approach, Proceedings of the conference on Bluff Bodies Aerodynamics & Applications, 2008, Milano, Italy.
46. BAKER, C.J., CHELI, F., ORELLANO, A., PARADOT, N., PROPPE, C. and ROCCHI, D. Cross wind effects on road and rail vehicles, *Vehicle Systems Dynamics*, 2009, **47**, (8), pp 983–1022.
47. ANDERSSON, E., HAGGSTROM, J., SIMA, M. and STICHEL, S. Assessment of train-overturning risk due to strong cross-winds, Proceedings of the Institution of Mechanical Engineers Part F J Rail and Rapid Transit, 2004, 218, 213-223, 10.1243/095440904238938287.

48. O'NEIL, H. Gauge modelling of West Coast Main Line tilting trains, Proceedings of the Institution of Mechanical Engineers Part F J Rail and Rapid Transit, 2008, 222, 235-253, 10.1243/09544097JRRT151.
49. BOUFERROUK, A., BAKER, C.J., STERLING, M., O'NEIL, H. and WOOD, S. Calculation of the cross wind displacement of pantographs, Proceedings of the Conference on Bluff Body Aerodynamics and its Applications', Milano, Italy.
50. DIEDRICHS, B., EKEQUIST, M., STICHEL, S. and TENGSTRAND, H. Quasi-static modelling of wheel–rail reactions due to crosswind effects for various types of high-speed rolling stock, Proceedings of the Institution of Mechanical Engineers, *Part F J Rail and Rapid Transit Transit,* 2004, **218**, pp 133-148.
51. THOMAS, D., DIEDRICHS, B., BERG, M. and STICHEL, S. Dynamics of a high-speed rail vehicle negotiating curves at unsteady crosswind., 21st International Symposium on Dynamics of Vehicles on Roads and Tracks (IAVSD'09), 2009, Stockholm, Sweden.
52. CHELI, F., CORRADI, R., DIANA, G., RIPAMONTI, F., ROCCHI, D. and TOMASINI, G. Methodologies for assessing trains CWC through time-domain multibody simulations, Proceedings of the 12th International Conference on Wind Engineering, 2007, Cairns, Australia.
53. STERLING, M., BAKER, C.J., BOUFERROUK, A., O'NEIL, H., WOOD, S. and CROSBIE, E. An investigation of the aerodynamic admittances and aerodynamic weighting functions of trains, *J Wind Engineering and Industrial Aerodynamics*, 2009, **97**, pp 512–522.
54 BAKER, C.J. A framework for the consideration of the effects of crosswinds on trains, *J Wind Engineering and Industrial Aerodynamics,* 2014, **123**, pp 130–142.
55. DORIGATI, F. Rail vehicles in crosswinds; analysis of steady and unsteady aerodynamic effects through static and moving model tests, 2013, PhD thesis, University of Birmingham, Birmingham, UK.
56. BAKER, C.J. 'A meta-analysis of train crosswind aerodynamic force coefficient data', Proceedings 13th International Conference on Wind Engineering, 2011, Amsterdam, Holland.
57. SANQUER, S. and BARRÉ, C. Dufresne de Virel M. and Cléon L-M. Effect of cross winds on high-speed trains, *J Wind Engineering and Industrial Aerodynamics,* 2004*,* **92**, 535-545, 10.1016/j.jweia.2004.03.004
58. BOCCIOLONE, M., CHELI, F., CORRADI, R., MUGGIASCA, S. and TOMASINI, G. (2008) Crosswind action on rail vehicles: Wind tunnel experimental analysis, *J Wind Engineering and Industrial Aerodynamics,* 96, pp 584-610.
59. BAKER, C.J. 'Wind overturning study: Full scale and wind tunnel measurements to determine the aerodynamic force and moment parameters of Mark 3 and Class 390 vehicles – Overview Report, 2003,, Report to Railway Safety.
60. WCRM Probabilities of overturning of Class 390 and Class 221 in high winds on the WCML – Library of reference reports, documents and data, 2004, Network Rail W091-189-TS-REP-005001
61. BAKER, C.J. Ground vehicles in high cross winds – Part 1 Steady aerodynamic forces, *J Fluids and Structuresm*, 1991, **5**, pp 69-90.
62. PEARCE, W. and BAKER, C.J. Measurement of the unsteady crosswind forces and moments on ground vehicles, MIRA Conference on Vehicle Aerodynamics, 1998, Birmingham, UK.
63. CHEN, R., ZENG,Q., ZHONG, X., XIANG, J., GUO, X. and ZHAO, G. Numerical study on the restriction speed of train passing curved rail in cross wind, Science in China Series E: Technological Sciences, Springer, 2009, **52**, (7), pp 2037-2047.
64. ALAM, F. and WATKINS, S. Effects of Crosswinds on Double Stacked Container Wagons, 16th Australasian Fluid Mechanics Conference, 2007, Crown Plaza, Gold Coast, Australia.
65. DIEDRICHS, B. On computational fluid dynamics modelling of crosswind effects for high-speed rolling stock, Proceedings of the Institution of Mechanical Engineers, 2003, Part F: J Rail and Rapid Transit 217: 203, 10.1243/095440903769012902.
66. DIEDRICHS, B. Aerodynamic calculations of crosswind stability of a high speed train using control volumes of arbitrary polyhedral shape, Proceedings of the conference on Bluff Bodies Aerodynamics and its Applications, 2008, Milano, Italy.
67. SCHOBER, S., WEISE, M., ORELLANO, A., DEEG, P. and WETZEL, W. Wind tunnel investigation of an ICE 3 endcar on three standard ground scenarios, Proceedings of the conference on Bluff Bodies Aerodynamics and its Applications, 2008, Milano, Italy.
68. DIEDRICHS, B., SIMA, M., ORELLANO, A. and TENGSTRAND, H. Crosswind stability of a high-speed train on a high embankment, 2007, Proceedings of the Institution of Mechanical Engineers Part F, J Rail and Rapid Transit 221, 205-225, 10.1243/0954409JRRT126.
69. CHELI, F., RIPAMONTI, F., ROCCHI, D., TOMASINI, G. and TESTA, M. Risk analysis of cross wind on HS/HC Rome-Naples Railway Line, Proceedings of the conference on Bluff Bodies Aerodynamics and its Applications, 2008, Milano, Italy.

70. CHELI, F., CORRADI, R., ROCCHI, D., TOMASINI, G. and MAESTRINI, E. Wind tunnel tests on train scale models to investigate the effect of infrastructure scenario, *J Wind Engineering and Industrial Aerodynamics*, 2010, **98**, pp 353–362, 10.1016/j.jweia.2010.01.001.
71. BIERBOOMS, W. and CHENG, P.-W. Stochastic gust model for design calculations of wind turbines, *J Wind Engineering and Industrial Aerodynamics*, 2002, **90**, pp 1237–1251.
72. MASSON, E. and HOEFENER, L. Aerodynamics in the Open Air, Work Package 2, Cross wind issues, Final Report, 2008.
73. GAWTHORPE, R.G. Pressure comfort criteria for rail tunnel operations, 7th International Symposium on the Aerodynamics and Ventilation of Vehicle Tunnels, 1991, 173-188, Brighton, UK.
74. JOHNSON, T., PREVEZER, T. and FIGURA-HARDY, G. Tunnel pressure comfort limits examined using passenger comfort ratings, 2000, Proceedings of the 10th International Symposium on Aerodynamics and Ventilation of Vehicle Tunnels Boston, USA.
75. VARDY, A.E. Generation and alleviation of sonic booms from rail tunnels, Proceedings of the Institution of Civil Engineers – Engineering and Computational Mechanics, 2008, **161**, (3), pp 107 –119.
76. HIEKE, M., GERBIG, C., TIELKES, T. and DEEG, P. Mastering Micro-pressure wave effects: Countermeasures at the Katzenberg Tunnel and Introduction of a new German regulation to get micro-pressure wave emissions under control, International Workshop on Train Aerodynamics, 2013, Birmingham, UK.
77. HIEKE, M., GERBIG, C., TIELKES, TH, K. and DEGEN, G. Assessment of micro-pressure wave emissions from high-speed railway tunnels, Proceedings of the World Congress on Rail Research, 2011, Lille, France.
78. TALOTTE, C., GAUTIER, P.-E., THOMPSON, D.J. and HANSON, C. Identification, modelling and reduction potential of railway noise sources: a critical survey, *J Sound and Vibration*, 2003, **267**, (I3), pp 447–468.
79. TIELKES, TH Aerodynamic Aspects of Maglev Systems, MAGLEV'2006: Proceedings of the 19th International Conference on Magnetically Levitated Systems and Linear Drives, 2006, Dresden, Germany
80. YAN, L. Development and Application of the Maglev Transportation System, Applied Superconductivity, 2008, IEEE Transactions 18, 2, 92-99, 10.1109/TASC.2008.922239.
81. GUSTAFSSON, M., BLOMQVIST, G., HÅKANSSON, K., LINDEBERG, J. and NILSSON-PÅLEDAL, S. Railway pollution – sources, dispersion and measures. A literature review, Swedish National Road and Transport Research Institute (VTI), Report 602, ISSN: 0347-6030.
82. LASSY, R., WIENER, L., HAGENA, B., RODLER, J., GRUNER, G. and GUTH, D. Dust in railway tunnels: Causes, Risks and Counter-measures, 2011, STUVA Convention 2011.
83. FERREIRA, A.D. and VAZ, P.A. Wind tunnel study of coal dust release from train wagons, *J Wind Engineering and Industrial Aerodynamics,* 2004, **92**, (5), pp 65-577.
84. JOHNSON, T. Development of a pantograph sway probability model, International Workshop on Train aerodynamics, 2013, Birmingham, UK.
85. GUO, W., XIA, H. and XU, Y. Dynamic response of a long span suspension bridge and running safety of a train under wind action, Frontiers of Architecture and Civil Engineering China, 2007, 1, 1, 71–79 10.1007/s11709-007-0007-1.
86. XU, Y.L., ZHANG, N. and XIA, H. Vibration of coupled train and cable-stayed bridge systems in cross winds, *Engineering Structures*, 2004, **26**, pp 1389–1406.
87. TAKEUCHI, T., MAEDA, J. and KAWASHITA, H. The overshoot of aerodynamic forces on a railcar-like body under step-function-like gusty winds, Proceedings of the conference on Bluff Bodies Aerodynamics and its Applications, 2008, Milano, Italy.